Converting non-periodic tilings with Tile$(1, 1)$ into tilings with three types of pentagons, II

Teruhisa SUGIMOTO[1),2)]

[1)] The Interdisciplinary Institute of Science, Technology and Art
[2)] Japan Tessellation Design Association
E-mail: ismsugi@gmail.com

Abstract

In the previous study [6], we demonstrated that non-periodic tilings generated using Tile$(1, 1)$ can be converted into non-periodic tilings with three types of pentagons. However, these results excluded the case where the conversion is performed after subdividing the original rhombus into smaller similar rhombuses. In this manuscript, we examine the case in which the conversion is performed after subdividing the original rhombus into smaller similar rhombuses. We describe the similarities and differences between the pentagonal tilings obtained by conversion with and without subdivision of the original rhombus into smaller similar rhombuses.

Keywords: pentagon, rhombus, tiling, non-periodic, aperiodic

1 Introduction

In this study, the non-periodic tiling[1] that can be generated using the clusters H_7 and H_8 in conjunction with the substitution method, as described in [2], is defined as T_h. The non-periodic tiling that can be generated using the clusters in conjunction with the substitution method, as described in the Appendix of [3], is defined as T_s.

As shown in the previous paper [6], if Tile$(1, 1)$ is assigned a pattern incorporating decomposition lines, as shown in Figure 1-1, then T_h and T_s with Tile$(1, 1)$ can also be converted into non-periodic tilings consisting of squares, regular hexagons, and rhombuses with an acute angle of 30° (see Figures 1-2 and 1-3). Because a regular hexagon can be divided into three rhombuses with an acute angle of 60°, both T_h and T_s with Tile$(1, 1)$ can be converted into non-periodic tilings consisting of rhombuses with acute angles of 90°, 60°, and 30°. (Note: A rhombus with an acute angle of 90° is a square). However, the division of a regular hexagon (the orientation of rhombuses obtained by division) is not uniquely determined.

As demonstrated in [4] and [5], a rhombic edge-to-edge tiling[2] (i.e., an edge-to-edge tiling with rhombuses) can be converted into a pentagonal tiling (i.e., a tiling with pentagons)

[1]A tiling (or *tessellation*) of the plane is a collection of sets, called tiles, that cover the plane without gaps or overlaps, except for the boundaries of the tiles. The term "tile" refers to a topological disk, whose boundary is a simple closed curve [1]. A tiling exhibits *periodicity* if its translation by a non-zero vector coincides with itself; a tiling is considered periodic if it coincides with its translation by two linearly independent vectors. However, in this study, a tiling with periodicity is referred to as *periodic*, and a tiling without periodicity is referred to as *non-periodic*.

[2]An edge-to-edge tiling with polygons is defined as a tiling in which the vertices (corners) and edges (sides) of the polygons coincide with the vertices (points where three or more tiles meet) and edges of the tiling [1].

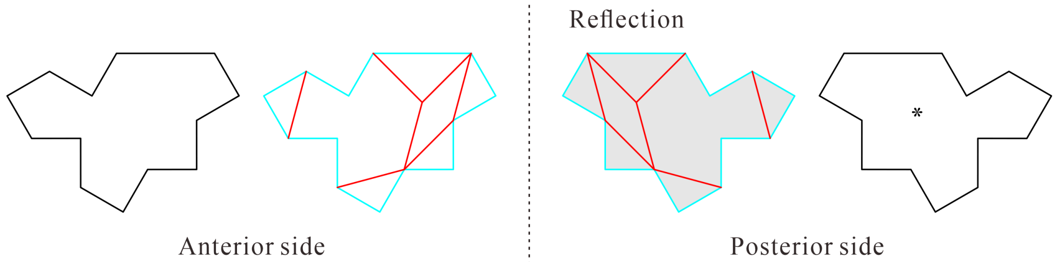

Figure 1-1: Tile$(1, 1)$ and Tile$(1, 1)$ with assigned decomposition lines.

using a specific method. In the previous paper [6], by studying this conversion method and non-periodic tilings T_h and T_s consisting of rhombuses with acute angles of 90°, 60°, and 30° based on the red line tilings in Figures 1-2 and 1-3, we confirmed that T_h and T_s with Tile$(1, 1)$ can be converted into non-periodic tilings with three types of pentagons. However, in [6], the case in which a tiling with rhombuses is converted into a tiling with pentagons after the original rhombus is divided such that it contains its own similar rhombuses (i.e., the original rhombus is subdivided into smaller similar rhombuses) was not considered. In this manuscript, we present the results of converting T_h and T_s with Tile$(1, 1)$ into pentagonal tilings after subdividing the original rhombus (i.e., a rhombus whose edge length is equal to the decomposition line assigned to Tile$(1, 1)$ in Figure 1-1) into smaller similar rhombuses. We then describe the similarities and differences between the pentagonal tilings obtained by conversion with and without subdivision of the original rhombus into smaller similar rhombuses.

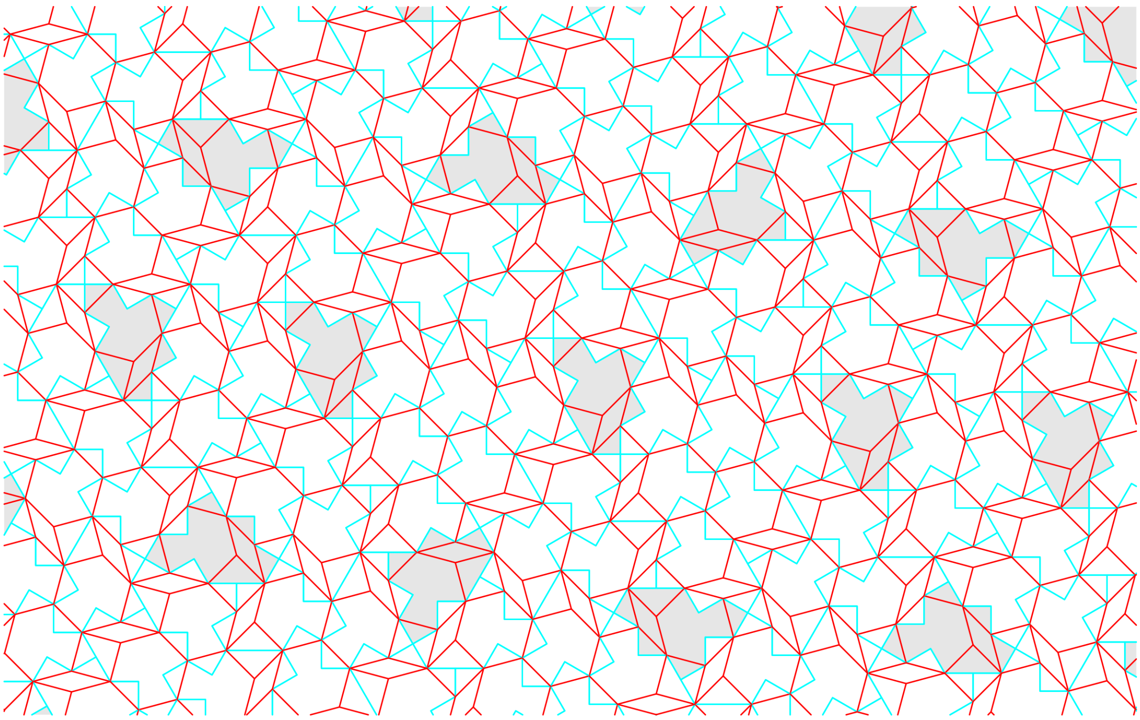

Figure 1-2: Conversion of the non-periodic tiling T_h with Tile$(1, 1)$ into a tiling consisting of squares, regular hexagons, and rhombuses with an acute angle of 30°.

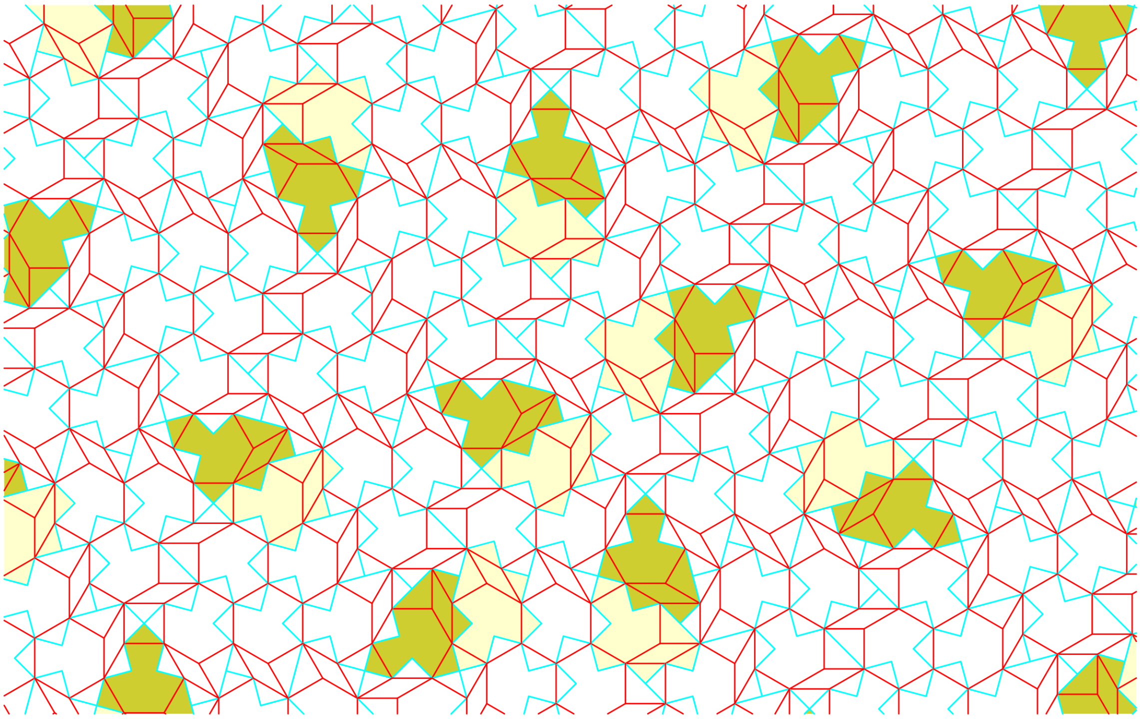

Figure 1-3: Conversion of the non-periodic tiling T_s with Tile$(1, 1)$ into a tiling consisting of squares, regular hexagons, and rhombuses with an acute angle of 30°.

2 Preparation

As in the previous paper [6], we first provide a brief review of the conversion of an edge-to-edge tiling with rhombuses into a tiling with pentagons, as presented in [4] and [5].

(i) An edge-to-edge tiling with rhombuses can be converted into a tiling with pentagons by converting one rhombus into two pentagons (a pair of pentagons)[3], as shown in Figure 2-1.

(ii) Because a rhombus can be divided into its own similar figures, a tiling with rhombuses can be converted into a tiling with pentagons after the original rhombus is divided such that it contains $4 \cdot u^2$ for $u = 1, 2, 3, \ldots$ of its own similar rhombuses.

(iii) The conversion of a tiling consisting of rhombuses with acute angles of 90°, 60°, and 30° into a pentagonal tiling can be performed using the contents of Section 5.3 in [5]. Depending on the value of the parameter θ, seven patterns (Sections 5.3.1 to 5.3.7 in [5]) with different combinations of three types of pentagons are realizable.

[3] The pentagons used in this conversion are *monotiles* (i.e., tiles that admit a *monohedral* tiling in which all tiles in a tiling are of the same size and shape). In monohedral tilings that allow the use of reflected tiles, the anterior and posterior sides of the tiles are treated as the same type (i.e., the concept assumes that there is only one type of tile). If the pentagons used in this conversion are convex, they are classified as convex pentagonal monotiles belonging to the Type 2 family [1, 4, 5]. The outline of this pair of pentagons can be regarded as a parallel equilateral concave octagon (a concave octagon in which all four pairs of opposite edges are parallel and all edges are of equal length). In other words, it can be regarded as a rhombus transformed into a parallel equilateral concave octagon that can generate a tiling by translation.

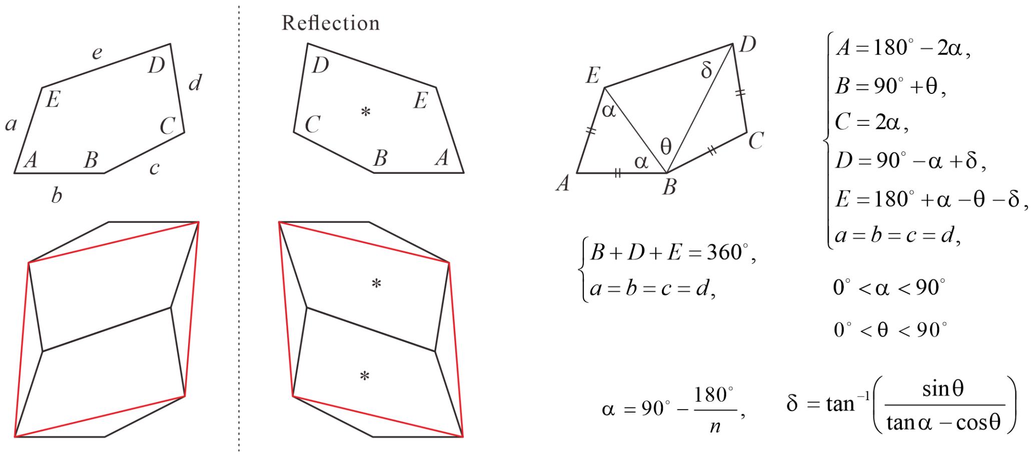

Figure 2-1: Properties of the pentagon used in the conversion, and the relationships between the rhombus and the pair of pentagons (pentagonal pair).

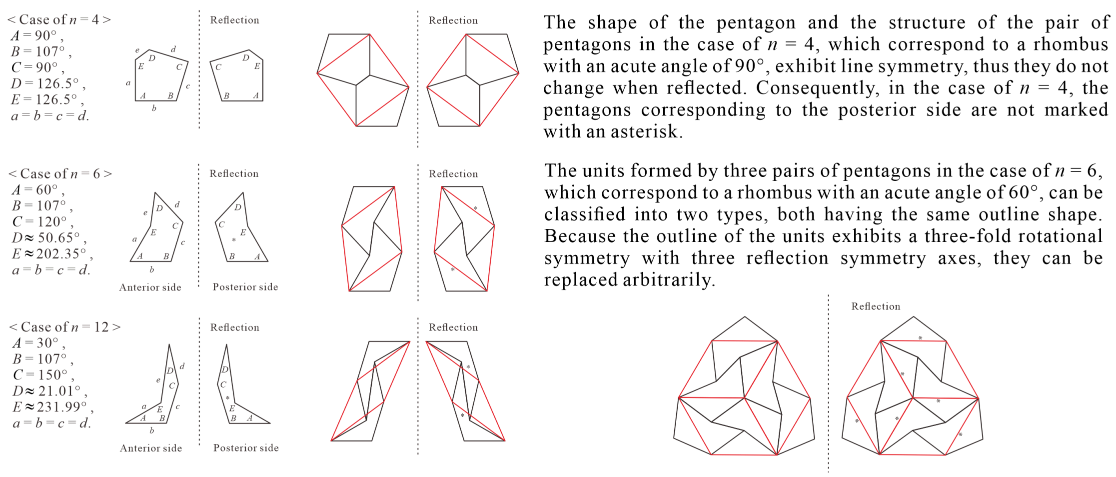

Figure 2-2: Pentagons used for the conversion in this study.

In this study, the three types of pentagons shown in Figure 2-2, derived from Section 5.3.1 ($\theta = 17^\circ$ in Table 5.3.1, i.e., $B = 107^\circ$) of [5], were used for the conversions. In other words, the following conversions were applied:

- Convert the rhombus with an acute angle of 90° into a pair of convex pentagons.
- Convert the rhombuses with acute angles of 30° and 60° into pairs of concave pentagons.

Therefore, the non-periodic tilings T_h and T_s are converted into tilings with one type of convex pentagon and two types of concave pentagons. Owing to the properties of the conversion method, conversions of other patterns that vary depending on the parameter θ, such as conversions using three types of convex pentagons, can also be obtained in the same way as the conversions performed in this study [5, 7, 8].

The orientation of rhombuses with an acute angle of 60°, obtained by dividing a regular hexagon into three sections, can be classified into two types and can be replaced arbitrarily.

A rhombus with an acute angle of 60° appears if and only if a regular hexagon is divided into three; however, no rule in this conversion has been identified that determines the orientation of the rhombuses obtained by dividing a regular hexagon into three sections. In the pentagonal tilings obtained by conversion in this study, this arbitrary replacement corresponds to swapping a unit formed by three pairs of pentagons on the anterior side and a unit formed by three pairs of pentagons on the posterior side (i.e., reflection). (As shown in Figure 2-2, because the outlines of the units are isomorphic and exhibit three-fold rotational symmetry with three reflection symmetry axes, the units can be replaced arbitrarily). In this study, during the conversion without subdivision of the original rhombus into smaller similar rhombuses (i.e., in the case where the original rhombus is not subdivided into smaller similar rhombuses), the arbitrary replacement is not performed, and all pentagons corresponding to the regular hexagon were on the anterior side (i.e., pentagons marked without asterisks in Figure 2-2) [6].

Next, we show examples related to the main purpose of this paper, such as case (ii), in which a tiling with rhombuses is converted into a tiling with pentagons after the original rhombus is divided such that it contains its own similar rhombuses. Figure 2-3 shows the case in which each original rhombus is divided into four smaller rhombuses by similarity division, and the resulting rhombus patches are converted into pentagonal patches (case (ii) with $u = 1$, where each patch contains eight pentagons). Figure 2-4 shows the case in which each original rhombus is divided into 16 smaller rhombuses by similarity division, and the resulting rhombus patches are converted into pentagonal patches (case (ii) with $u = 2$, where each patch contains 32 pentagons).

As mentioned in the previous paper [6], the patterns on Tile(1, 1) for forming each pattern of the pentagonal tilings (i.e., the patterns created by the decomposition lines corresponding to each pentagonal tiling) corresponding to T_h and T_s can be classified into multiple types. In this study, we do not classify Tile(1, 1) based on different patterns, nor do we use different patterns of Tile(1, 1) to generate tilings. The conversion results in this study can be obtained by generating tilings using clusters, in conjunction with the substitution method described in [2] and [3].

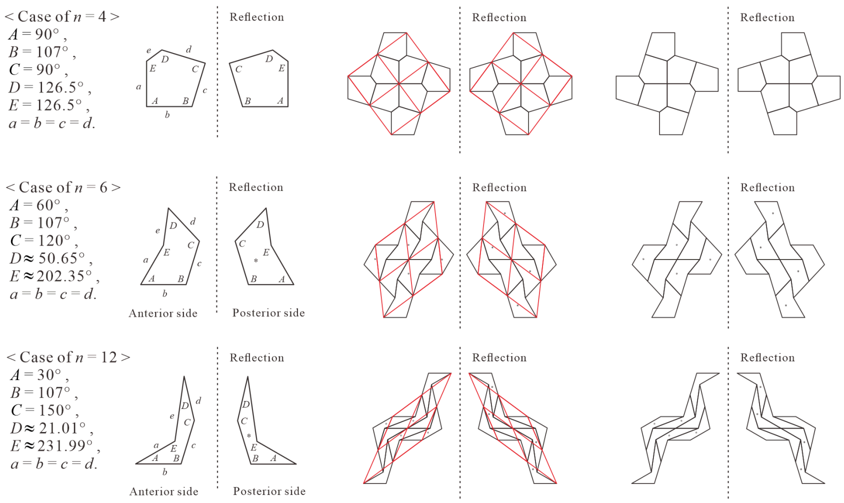

Figure 2-3: Case in which each original rhombus is divided into four smaller rhombuses by similarity division, and the resulting rhombus patches are converted into pentagonal patches.

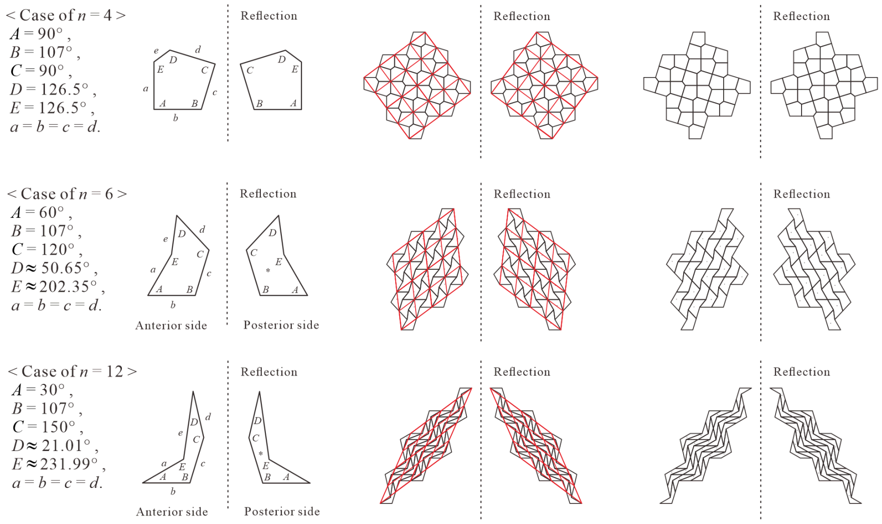

Figure 2-4: Case in which each original rhombus is divided into 16 smaller rhombuses by similarity division, and the resulting rhombus patches are converted into pentagonal patches.

Most of the related figures in this manuscript illustrating the conversion of T_h and T_s with Tile$(1, 1)$ into pentagonal tilings after subdividing the original rhombus into smaller similar rhombuses are for the cases of $u = 1$ and $u = 2$. Therefore, the figures in this manuscript primarily depict clusters formed with three types of pentagons to generate T_h and T_s for the cases of $u = 1$ and $u = 2$. Note that drawing tilings in the cases of $u = 1$ and $u = 2$, corresponding to Figures 1-2 and 1-3, is currently difficult due to PC specification constraints. Furthermore, in the case of $u \geq 3$, clusters can be formed with pentagonal patches in the same manner, and tilings can be generated. However, drawing these tilings is even more difficult due to PC specification constraints.

3 Pentagonal patches on AO-side and PO-side

When a rhombus is converted into two pentagons (a pair of pentagons), as shown in Figure 2-2, there are pentagonal patches formed exclusively by pentagons of the anterior side (marked without an asterisk) and pentagonal patches formed exclusively by pentagons of the posterior side (marked with an asterisk). On the other hand, when a rhombic patch, obtained by subdividing the original rhombus into smaller similar rhombuses, is converted into pentagons, as shown in Figures 2-3 and 2-4, the resulting pentagonal patches corresponding to the original rhombus contain pentagons on both the anterior and posterior sides.

In the following, the case where the original rhombus is not subdivided into smaller similar rhombuses is referred to as the "case of $u = 0$," and the case where it is subdivided is referred to as the "case of $u \geq 1$."

In this study, after considering the results of the conversion in the cases of $u = 0$ and $u \geq 1$, we define the case where pentagons on the **a**nterior side are placed at the **o**btuse angles of rhombuses as the "AO-side" and the case where pentagons on the **p**osterior side are placed at the **o**btuse angles of rhombuses as the "PO-side" (see Figure 3-1). Note that in a rhombus with an acute angle of 90°, i.e., a square, there is no distinction between acute and obtuse angles, and the corresponding pentagon also does not distinguish between the anterior and posterior sides because it exhibits line symmetry. However, the AO-side and PO-side of these patches were determined based on the case of other rhombuses.

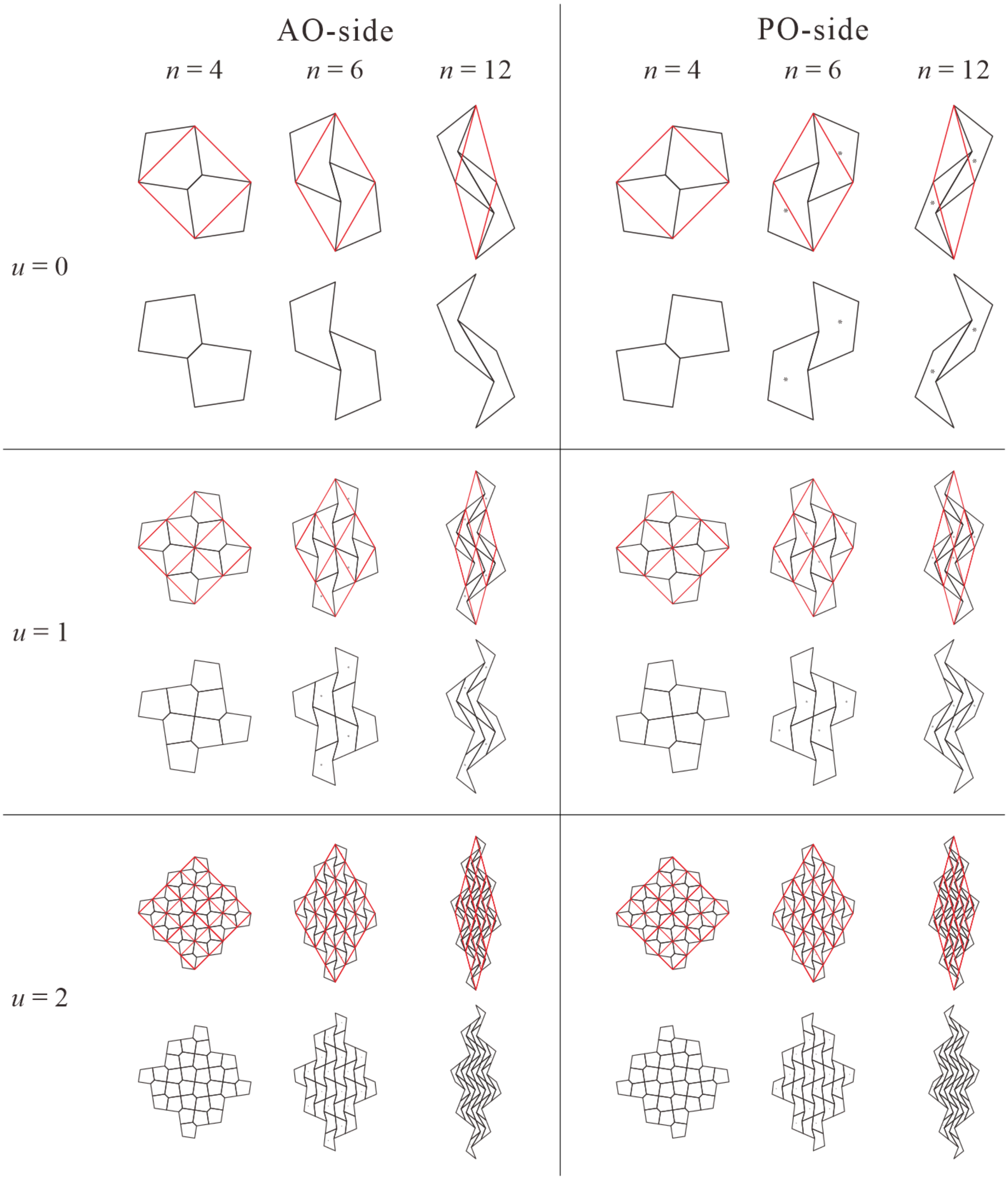

Figure 3-1: Pentagonal patches on the AO-side and PO-side corresponding to the three types of rhombuses.

When a rhombus with an acute angle of 90° (a square) is converted into pentagons without subdivision of the rhombus into smaller similar rhombuses, as in the case of $u = 0$ in Figure 3-1, the pentagonal patches on the AO-side and PO-side exhibit two-fold rotational symmetry with two reflection symmetry axes and are isomorphic[4]. On the other hand, when a rhombus with an acute angle of 90° is converted into pentagons after being subdivided into smaller similar rhombuses, as in the cases of $u = 1$ and $u = 2$ in Figure 3-1, the resulting pentagonal patches on the AO-side and PO-side corresponding to the original rhombus exhibit four-fold rotational symmetry without reflection symmetry axes and are reflected images of each other (i.e., they cannot be replaced).

AO-side in Figure 3-2 shows AO-side pentagonal patches corresponding to an original regular hexagon (a regular hexagon whose edge length is equal to the decomposition line assigned to Tile(1, 1) in Figure 1-1), which are formed by three AO-side pentagonal patches associated with a rhombus with an acute angle of 60°. PO-side in Figure 3-2 shows PO-side pentagonal patches corresponding to an original regular hexagon, which are formed by three PO-side pentagonal patches associated with a rhombus with an acute angle of 60°. The outlines of the pentagonal patches corresponding to the original regular hexagon in the case of $u = 0$ are isomorphic and exhibit a three-fold rotational symmetry with three reflection symmetry axes. On the other hand, the outlines of the pentagonal patches corresponding to the original regular hexagon in the case of $u \geq 1$ exhibit a six-fold rotational symmetry without reflection symmetry axes. As shown in Figure 3-3, when each pentagonal patch corresponding to the original regular hexagon in the case of $u \geq 1$ is rotated by 60°, its outline remains unchanged, but the arrangement of the internal pentagons changes. When it is rotated by another 60° (120° from the original arrangement), the arrangement of the internal pentagons is identical to its initial state. (That is, each pentagonal patch corresponding to the original regular hexagon in the case of $u \geq 1$ exhibits a three-fold rotational symmetry). One type of arbitrary replacement of pentagonal patches corresponding to regular hexagons[5] in the case of $u \geq 1$ is a change in the arrangement of the internal pentagons caused by this rotation. The outlines of the pentagonal patches on the AO-side and PO-side, corresponding to the regular original hexagon in the case of $u \geq 1$, are reflected images of each other but do not exhibit line symmetry. Therefore, unlike in the case of $u = 0$, these patches cannot be replaced.

Furthermore, as shown in Figures 3-4–3-6, in the case of $u \geq 1$, the replacement of units formed by three pairs of pentagons on the anterior side and units formed by three pairs of pentagons on the posterior side, corresponding to regular hexagons that appear within pentagonal patches corresponding to the original regular hexagon, is allowed. Consequently, pentagonal patches corresponding to the original regular hexagon with a variety of patterns (design patterns created by the arrangement of polygonal tiles) can be created. The ability to generate (and use) these various patterns is also an arbitrary replacement of locations (pentagonal patches) corresponding to regular hexagons in the case of $u \geq 1$.

In this study, arbitrary replacements of locations corresponding to regular hexagons are not performed during the conversion. Each pentagonal patch corresponding to the original regular hexagon in the case of $u \geq 1$ always follows a pattern formed by three pentagonal patches corresponding to a rhombus with an acute angle of 60°, as shown in Figure 3-2.

In the case of $u \geq 1$, for the pentagonal patches corresponding to the original regular hexagon, as shown in Figure 3-2, we observe that the pentagons at the vertices of the original

[4]The pentagon used in the conversion of a square and the resulting pair of pentagons exhibit line symmetry, meaning there is no distinction between the anterior and posterior sides. Therefore, these pentagons corresponding to the posterior side are not marked with asterisks.

[5]As mentioned in Section 2, the orientation of rhombuses with an acute angle of 60°, obtained by dividing a regular hexagon into three sections, can be classified into two types and can be replaced arbitrarily.

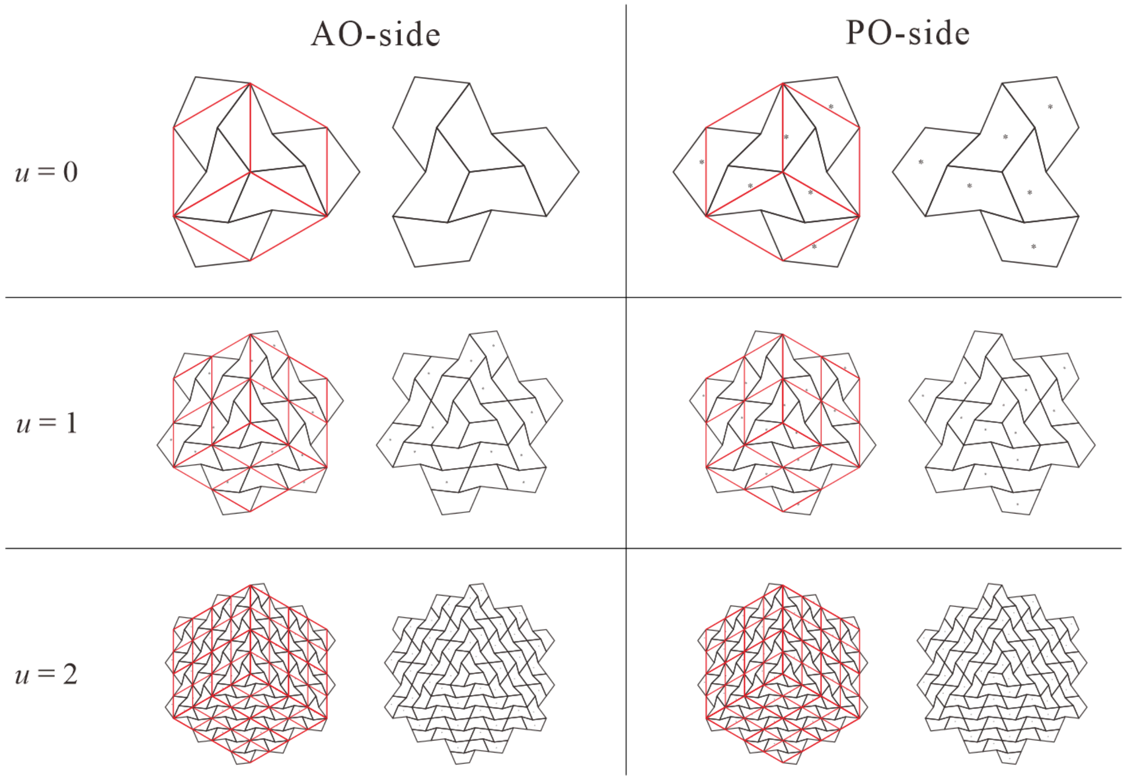

Figure 3-2: Pentagonal patches on the AO-side and PO-side corresponding to an original regular hexagon formed by three pentagonal patches associated with rhombus with an acute angle of 60°.

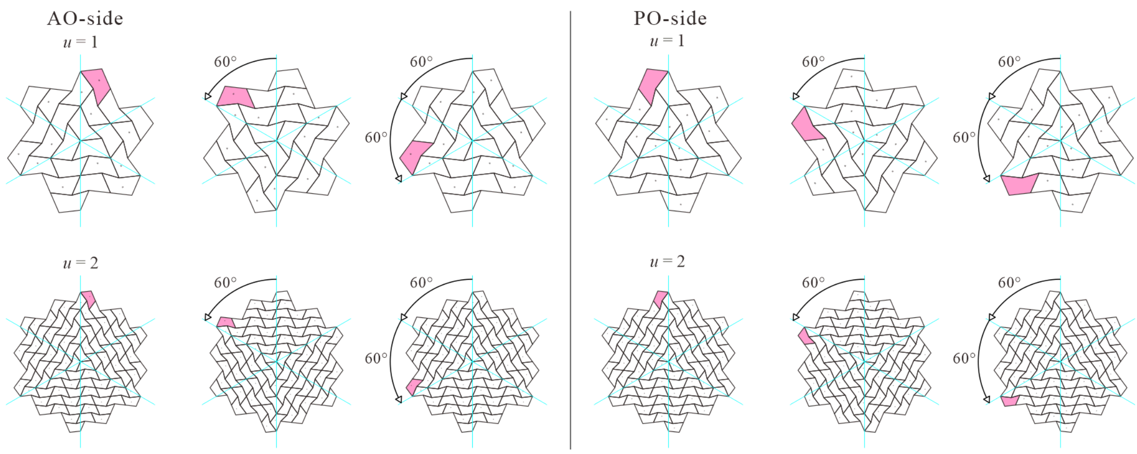

Figure 3-3: Pentagonal patches corresponding to an original regular hexagon rotated by 60° and 120°.

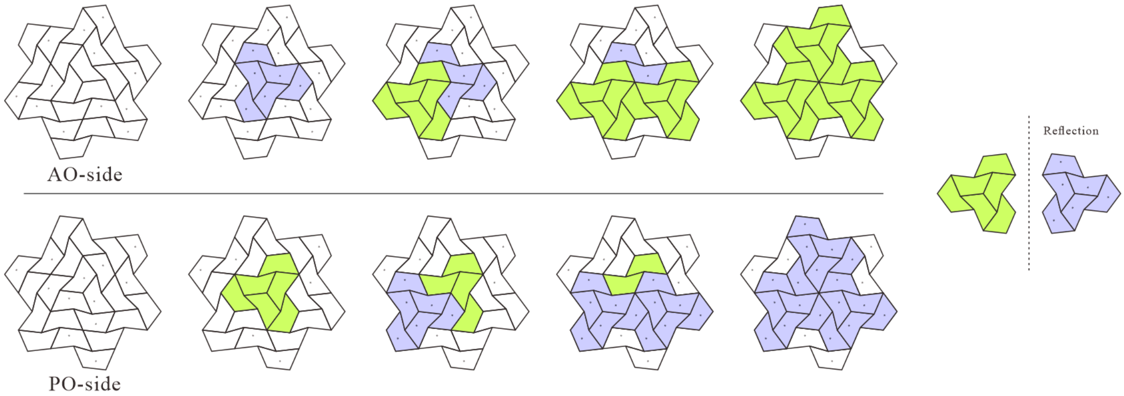

Figure 3-4: Patterns of pentagonal patches corresponding to an original regular hexagon in the case of $u = 1$.

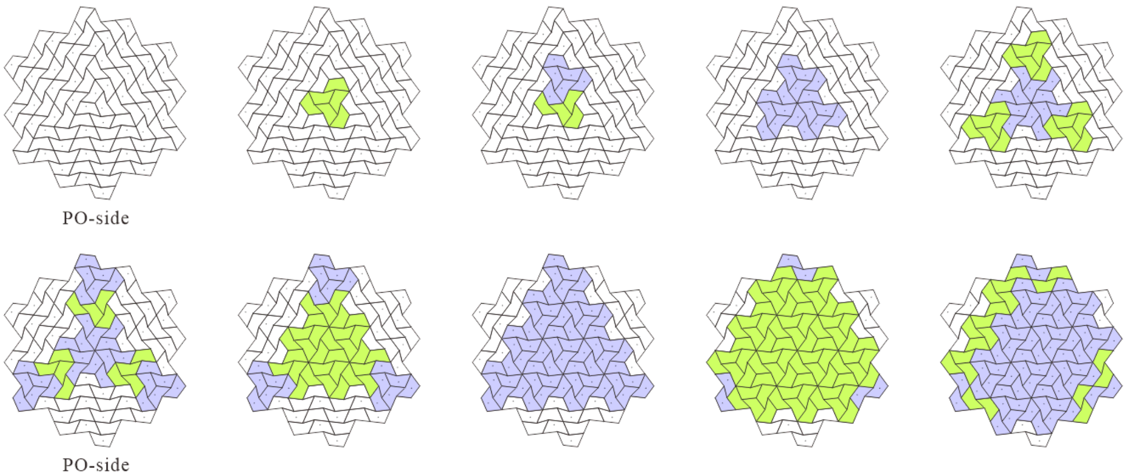

Figure 3-5: Examples of patterns of pentagonal patches corresponding to an original regular hexagon in the case of $u = 2$.

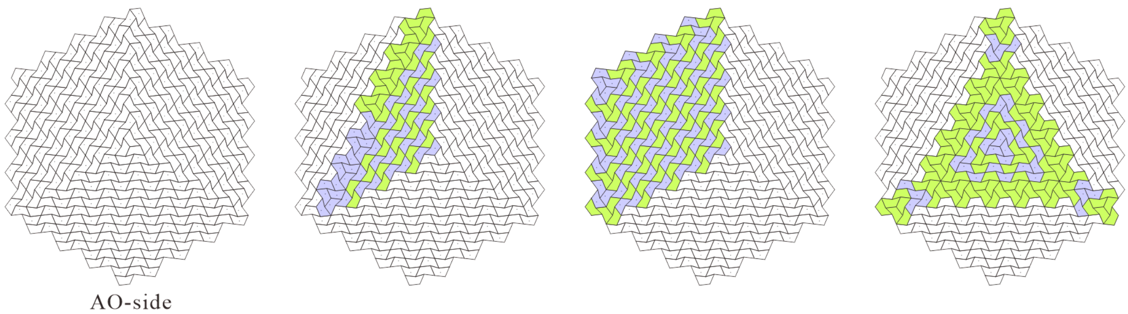

Figure 3-6: Examples of patterns of pentagonal patches corresponding to an original regular hexagon in the case of $u = 3$.

regular hexagon alternate between the anterior and posterior sides, with each side. As shown in Figure 3-4, in the case of $u = 1$, all pentagons forming the AO-side pentagonal patch corresponding to the original regular hexagon can be on the anterior side (marked without asterisks) but cannot be on the posterior side. In contrast, in the case of $u = 1$, all pentagons forming the PO-side pentagonal patch corresponding to the original regular hexagon can be on the posterior side (marked with asterisks) but cannot be on the anterior side. On the other hand, in the case of $u \geq 2$, we conjecture that all pentagons forming the pentagonal patches corresponding to the original regular hexagon cannot be exclusively on either the anterior or the posterior side (see Figures 3-5 and 3-6). However, for PO-side pentagonal patches corresponding to the original regular hexagon in the case of $u \geq 2$, we conjecture that all pentagons at the vertices of the original regular hexagon can be on the posterior side (see the pattern in the lower row of Figure 3-5) but cannot be on the anterior side. In contrast, for AO-side pentagonal patches corresponding to the original regular hexagon in the case of $u \geq 2$, we conjecture that all pentagons at the vertices of the original regular hexagon can be on the anterior side (see the rightmost pattern in Figure 3-6) but cannot be on the posterior side.

4 Conversion of non-periodic tiling T_h

In this section, we combine the conversion results in the case of $u = 0$, presented in Section 3 of the previous paper [6], into those in the case of $u \geq 1$, and reconsider the case in which T_h with Tile(1, 1) is converted into pentagonal tilings. As a result, when arbitrary replacements of locations corresponding to regular hexagons are excluded, we can observe two patterns of non-periodic tilings with three types of pentagons corresponding to T_h with Tile(1, 1), and we present the properties of these patterns.

In this study, the conversion results were obtained by generating tilings using clusters H_8 and H_7, in conjunction with the substitution method presented in [2]. Thus, non-periodic tilings with three types of pentagons can be generated using clusters composed of three types of pentagons, based on H_8 and H_7 formed by Tile(1, 1) (see Figure 4-1), in conjunction with the substitution method for H_8 and H_7 described in [2].

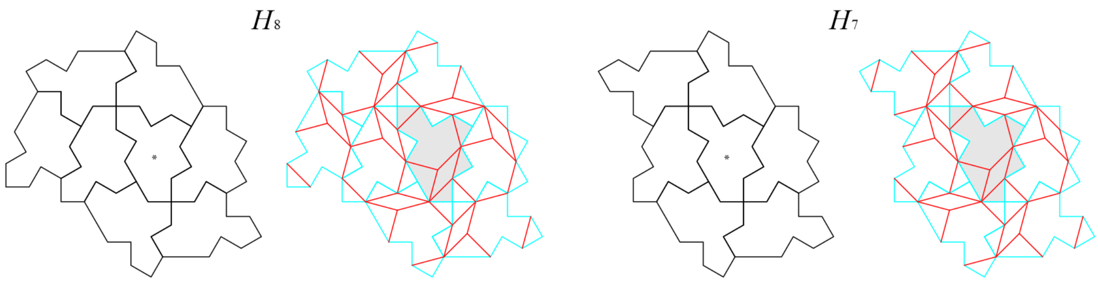

Figure 4-1: Clusters H_8 and H_7 formed by Tile(1, 1).

4.1 First pattern of T_h

The first pattern of T_h (the first pattern when T_h with Tile(1, 1) is converted into a tiling with three types of pentagons) is generated by placing PO-side pentagonal patches on the original rhombuses. For the conversion in the case of $u = 0$, refer to Section 3.1 in [6]. Now,

$FPH_8(2,1)$ $FPH_7(2,1)$

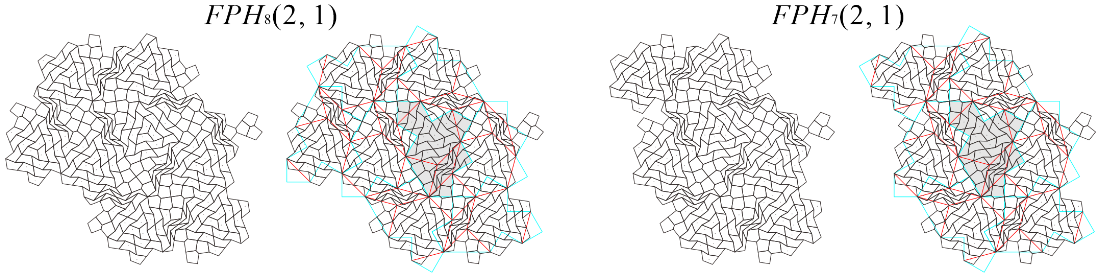

Figure 4-2: $FPH_8(2,1)$ and $FPH_7(2,1)$.

$FPH_8(2,2)$ $FPH_7(2,2)$

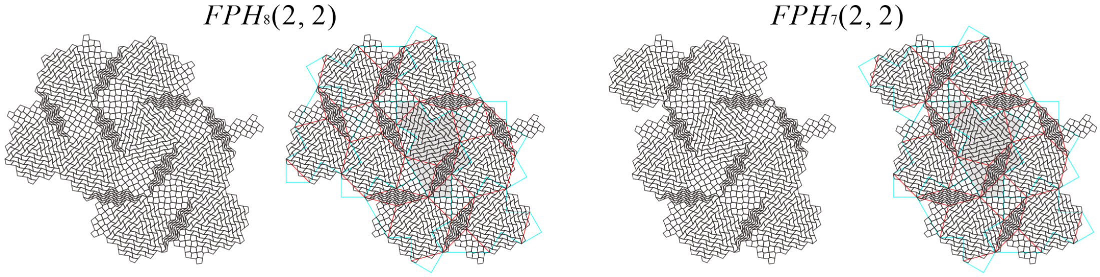

Figure 4-3: $FPH_8(2,2)$ and $FPH_7(2,2)$

let $FPH_8(2,u)$ and $FPH_7(2,u)$ denote the clusters of the first pattern in the case of $u \geq 1$, formed by three types of pentagons based on H_8 and H_7 (Figure 4-1). Figure 4-2 presents the clusters $FPH_8(2,1)$ and $FPH_7(2,1)$ in the case of $u = 1$, while Figure 4-3 presents the clusters $FPH_8(2,2)$ and $FPH_7(2,2)$ in the case of $u = 2$.

Figure 4-4 shows the clusters $FPH_8(2)$ (in the case of $u = 0$, see Figure 3-2 in [6]), $FPH_8(2,1)$ (in the case of $u = 1$, see Figure 4-2), and $FPH_8(2,2)$ (in the case of $u = 2$, see Figure 4-3), which are formed by three types of pentagons based on H_8. The regions along the contours of these clusters that correspond to the original rhombuses with an acute angle of 90° (which contain only half the number of pentagons) are highlighted in light blue. From Figure 4-4, it is seen that the orientations (contact configurations) of the pentagons in the light blue regions share a common property. Non-periodic tilings generated by clusters exhibiting this common property are classified into the first pattern of T_h.

Thus, by focusing on the common properties between the cases of $u = 0$ and $u \geq 1$, we assume that the first pattern of T_h represents the case in which the pentagons on the posterior side can be placed at the obtuse angles of the rhombuses (i.e., PO-side pentagonal patches can be placed on the original rhombuses)[6].

For the first pattern of T_h with three types of pentagons in the case of $u = 0$, see Figure 3-4 in [6]. Owing to PC specifications and other constraints, it is currently difficult to present figures (equivalent to Figure 3-4 in [6]) depicting the first pattern of T_h with three types of pentagons in the case of $u \geq 1$. Therefore, in Figure A-1 of Appendix A, we provide two types

[6]Owing to this property, in both cases of $u = 0$ and $u = 1$, if PO-side pentagonal patches are placed on the original rhombuses with an acute angle of 30°, the first pattern of T_h can be generated. We use the phrase "pentagons (patches) can be placed" because we consider the fact that pentagons corresponding to the rhombus with an acute angle of 90° exhibit line symmetry, as well as the fact that the replacement of units formed by three pairs of pentagons on the anterior side and units formed by three pairs of pentagons on the posterior side corresponding to regular hexagons is allowed.

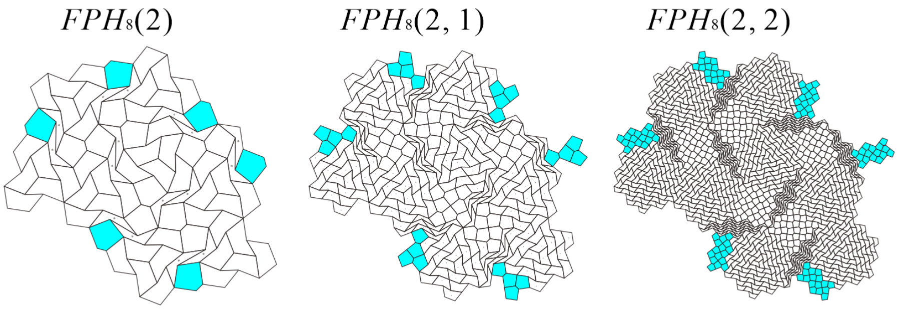

Figure 4-4: Regions on the contours of $FPH_8(2)$, $FPH_8(2,1)$, and $FPH_8(2,2)$ corresponding to the original rhombuses with an acute angle of 90°.

of concave polygons equivalent to the outlines of $FPH_8(2,1)$ and $FPH_7(2,1)$, and present clusters corresponding to $FPH_8(3,1)$ and $FPH_8(4,1)$ (i.e., the next substitution step and its next step clusters) using these polygons.

4.2 Second pattern of T_h

The second pattern of T_h (the second pattern when T_h with Tile(1, 1) is converted into a tiling with three types of pentagons) is generated by placing AO-side pentagonal patches on the original rhombuses. For the conversion in the case of $u = 0$, refer to Section 3.2 in [6]. Now, let $SPH_8(2,u)$ and $SPH_7(2,u)$ denote the clusters of the second pattern in the case of $u \geq 1$, formed by three types of pentagons based on H_8 and H_7 (Figure 4-1). Figure 4-5 presents the clusters $SPH_8(2,1)$ and $SPH_7(2,1)$ in the case of $u = 1$, while Figure 4-6 presents the clusters $SPH_8(2,2)$ and $SPH_7(2,2)$ in the case of $u = 2$.

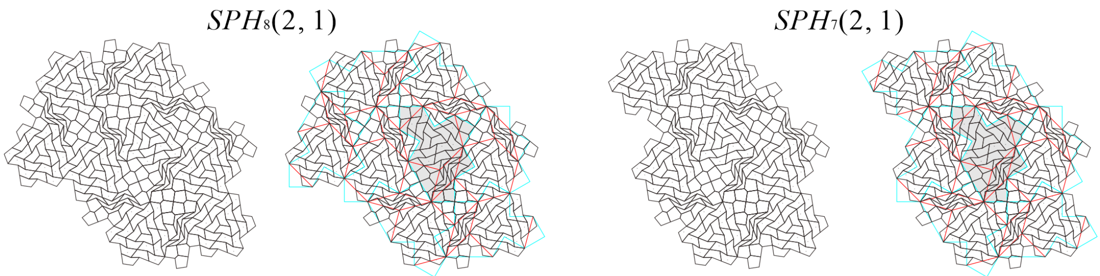

Figure 4-5: $SPH_8(2,1)$ and $SPH_7(2,1)$.

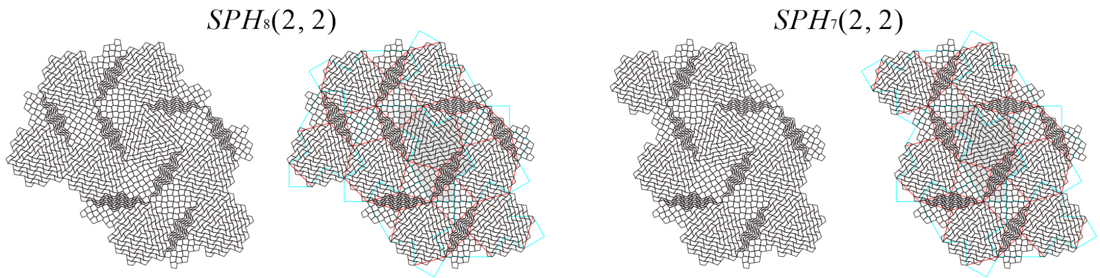

Figure 4-6: $SPH_8(2,2)$ and $SPH_7(2,2)$

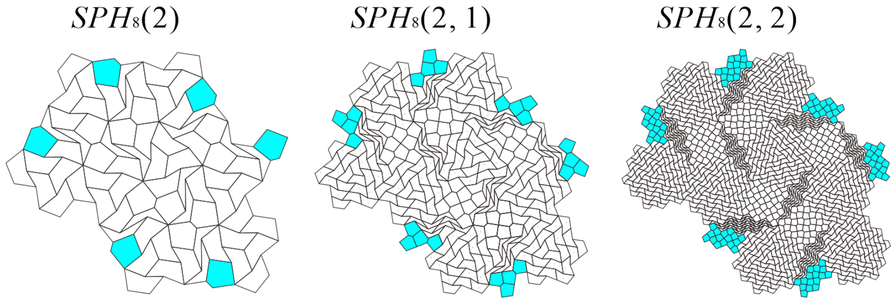

Figure 4-7: Regions on the contours of $SPH_8(2)$, $SPH_8(2,1)$, and $SPH_8(2,2)$ corresponding to the original rhombuses with an acute angle of 90°.

Figure 4-7 shows the clusters $SPH_8(2)$ (in the case of $u = 0$, see Figure 3-5 in [6]), $SPH_8(2,1)$ (in the case of $u = 1$, see Figure 4-5), and $SPH_8(2,2)$ (in the case of $u = 2$, see Figure 4-6), which are formed by three types of pentagons based on H_8. The regions along the contours of these clusters that correspond to the original rhombuses with an acute angle of 90° (which contain only half the number of pentagons) are highlighted in light blue. From Figure 4-7, it is seen that the orientations (contact configurations) of the pentagons in the light blue regions share a common property. Non-periodic tilings generated by clusters exhibiting this common property are classified into the second pattern of T_h.

Thus, by focusing on the common properties between the cases of $u = 0$ and $u \geq 1$, we assume that the second pattern of T_h represents the case in which the pentagons on the anterior side can be placed at the obtuse angles of the rhombuses (i.e., AO-side pentagonal patches can be placed on the original rhombuses)[7].

For the second pattern of T_h with three types of pentagons in the case of $u = 0$, see Figure 3-7 in [6]. Owing to PC specifications and other constraints, it is currently difficult to present figures (equivalent to Figure 3-7 in [6]) depicting the second pattern of T_h with three types of pentagons in the case of $u \geq 1$. Therefore, in Figure A-2 of Appendix A, we provide two types of concave polygons equivalent to the outlines of $SPH_8(2,1)$ and $SPH_7(2,1)$, and present clusters corresponding to $SPH_8(3,1)$ and $SPH_8(4,1)$ (i.e., the next substitution step and its next step clusters) using these polygons.

5 Conversion of non-periodic tiling T_s

In Sections 5.1–5.3, we show the properties of the conversion results of T_s in the case of $u \geq 1$, and indicate the difference from the properties of the conversion results of T_s in the case of $u = 0$ shown in the previous paper [6]. Note that, in both cases, when arbitrary replacements of locations corresponding to regular hexagons are excluded, we can observe two patterns of non-periodic tilings with three types of pentagons corresponding to T_s with Tile(1, 1). In Section 5.4, by focusing on the common properties between the cases of $u = 0$ and $u \geq 1$, we show that if T_s with Tile(1, 1) is converted into pentagonal tilings, allowing arbitrary replacements of locations corresponding to the structure of Mystic (see explanation

[7]Owing to this property, in both cases of $u = 0$ and $u = 1$, if AO-side pentagonal patches are placed on the original rhombuses with an acute angle of 30°, the second pattern of T_h can be generated. The reason why for using the phrase "pentagons (patches) can be placed" is the same as that stated in footnote 6.

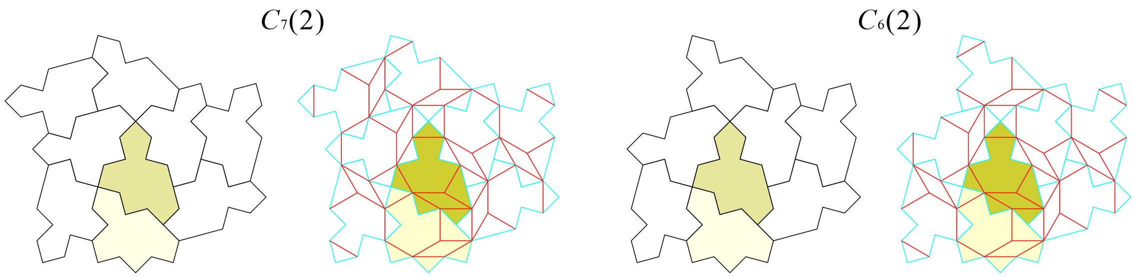

Figure 5-1: Clusters in Step 2 of Figure A.1 in [3].

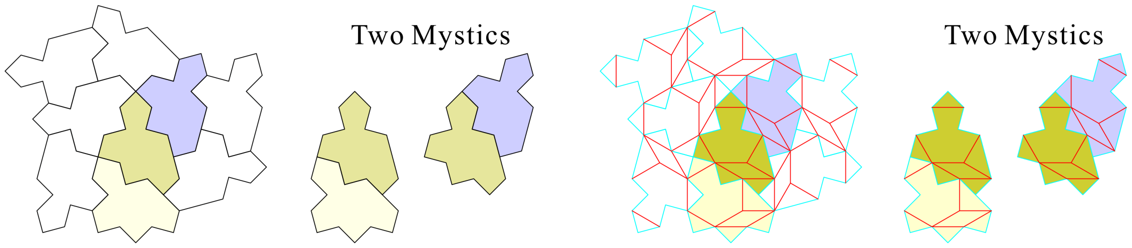

Figure 5-2: Two Mystic regions that formed by three Tile(1, 1) in $C_7(2)$.

below), two series of patterns emerge for non-periodic tilings with three types of pentagons corresponding to T_s with Tile(1, 1). We also describe the properties of these patterns.

In this study, the conversion results can be obtained by generating tilings using the cluster in Step 2a of Figure A.1 in [3] (see Figure 5-1, denoted as $C_7(2)$) and the cluster obtained by removing one Tile(1, 1) from $C_7(2)$ (see Figure 5-1, denoted as $C_6(2)$), in conjunction with the substitution method described in [3]. In other words, we can generate non-periodic tilings with three types of pentagons using the clusters composed of three types of pentagons based on $C_7(2)$ and $C_6(2)$ formed by Tile(1, 1), in conjunction with the substitution method for $C_7(2)$ and $C_6(2)$ shown in [3].

The structure formed by the two colored Tile(1, 1) in Figure 5-1 is referred to as the “Mystic” region in [3]. As shown in Figure 5-2, we assumed that two locations correspond to the Mystic structure in $C_7(2)$ (i.e., two Mystic regions formed by three Tile(1, 1)).

Based on the substitution method described in the Appendix of [3], the tiles are switched between the anterior and posterior sides (i.e., the tiles are reversed) at each substitution step. For example, if $C_7(3)$ corresponding to the cluster in Step 3 is formed by performing a substitution using clusters $C_7(2)$ and $C_6(2)$ in Figure 5-1, then all Tile(1, 1) in $C_7(3)$ will be at the posterior side in Figure 1-1. However, in the figures of this study, we have not adopted a notation to indicate that the tiles are reversed at each substitution step. We will adjust the figures so that Tile(1, 1) in the tilings and clusters will be oriented toward the anterior side shown in Figure 1-1.

5.1 First pattern of T_s

The first pattern of T_s (the first pattern when T_s with Tile(1, 1) is converted into a tiling with three types of pentagons) in the case of $u \geq 1$ is generated by placing PO-side pentagonal patches on the original rhombus. Let $FPC_7(2, u)$ and $FPC_6(2, u)$ denote the clusters of the first pattern in the case of $u \geq 1$, formed by three types of pentagons based on $C_7(2)$ and

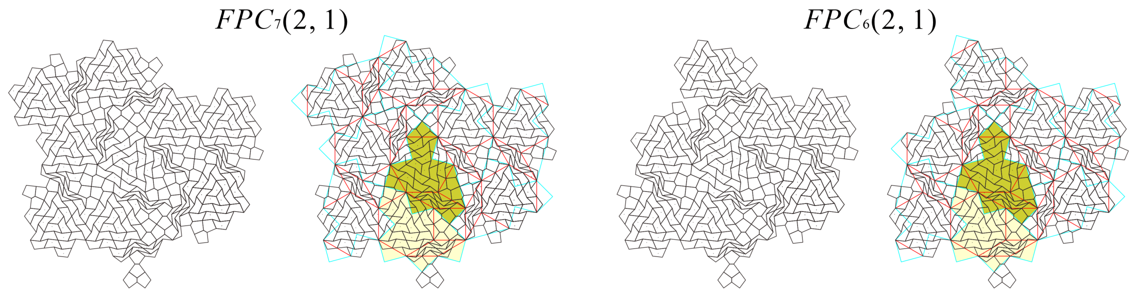

Figure 5-3: $FPC_7(2, 1)$ and $FPC_6(2, 1)$.

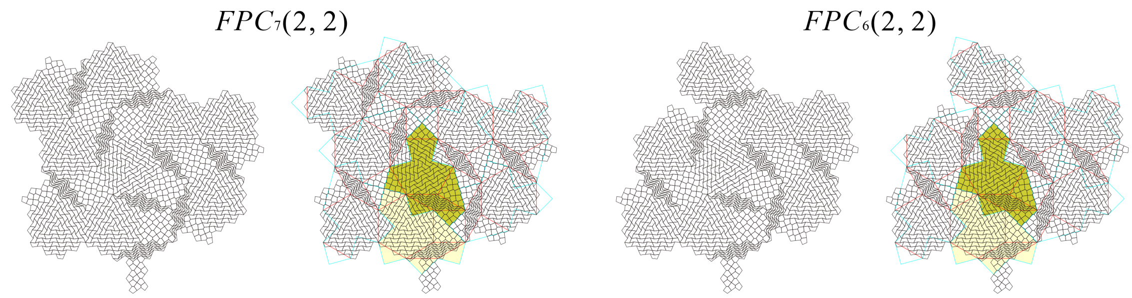

Figure 5-4: $FPC_7(2, 2)$ and $FPC_6(2, 2)$

$C_6(2)$ (Figure 5-1). Figure 5-3 presents the clusters $FPC_7(2, 1)$ and $FPC_6(2, 1)$ in the case of $u = 1$, while Figure 5-4 presents the clusters $FPC_7(2, 2)$ and $FPC_6(2, 2)$ in the case of $u = 2$.

The explanation of the first pattern of T_s in the case of $u = 0$ shown in [6] can be rewritten using the terms "AO-side" and "PO-side," as shown below. In the first pattern of T_s in the case of $u = 0$, the pentagonal patches (the pairs of pentagons) corresponding to the rhombus with an acute angle of 30° (see the rhombus with an orange filter in Figure 4-4 in [6]) within Tile(1, 1)[8], which appears in the overlap of two Mystic regions in $C_7(2)$ and $C_6(2)$, are the AO-side. Meanwhile, the other pentagonal patches corresponding to the remaining rhombuses with an acute angle of 30° are the PO-side. In other words, in the first pattern of T_s in the case of $u = 0$, PO-side pentagonal patches can be placed on most rhombuses[9], whereas AO-side pentagonal patches must be placed on some rhombuses with an acute angle of 30°.

In Section 5.4, wel explain the reason why Figures 5-3 and 5-4 represent the first pattern, from the same perspective as Figure 4-4 for T_h, and discuss the common properties of the first pattern series of T_s in the cases of $u = 0$ and $u \geq 1$.

5.2 Second pattern of T_s

The second pattern of T_s (the second pattern when T_s with Tile(1, 1) is converted into a tiling with three types of pentagons) in the case of $u \geq 1$ is generated by placing AO-side

[8] The overlapping Tile(1, 1) corresponds to the "odd tile" in [3].

[9] We use the phrase "patches can be placed" because, in the case of $u = 0$, we consider the fact that pentagonal patches corresponding to the rhombus with an acute angle of 90° are isomorphic, as well as the fact that pentagonal patches corresponding to regular hexagons can be replaced.

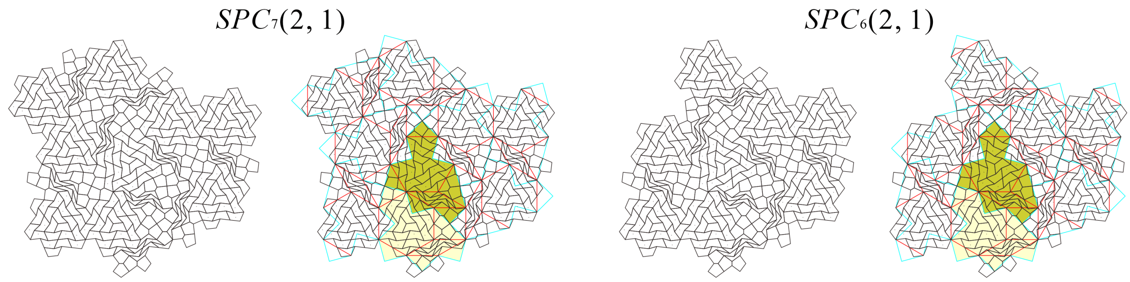

Figure 5-5: $SPC_7(2, 1)$ and $SPC_6(2, 1)$.

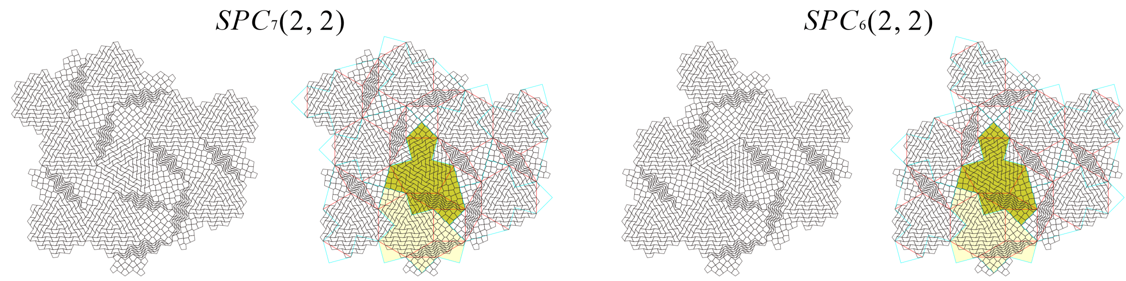

Figure 5-6: $SPC_7(2, 2)$ and $SPC_6(2, 2)$

pentagonal patches on the original rhombus. Let $SPC_7(2, u)$ and $SPC_6(2, u)$ denote the clusters of the second pattern in the case of $u \geq 1$, formed by three types of pentagons based on $C_7(2)$ and $C_6(2)$ (Figure 5-1). Figure 5-5 presents the clusters $SPC_7(2, 1)$ and $SPC_6(2, 1)$ in the case of $u = 1$, while Figure 5-6 presents the clusters $SPC_7(2, 2)$ and $SPC_6(2, 2)$ in the case of $u = 2$.

The explanation of the second pattern of T_s in the case of $u = 0$ shown in [6] can be rewritten using the terms "AO-side" and "PO-side," as shown below. In the second pattern of T_s in the case of $u = 0$, the pentagonal patches (the pairs of pentagons) corresponding to the rhombus with an acute angle of 30° within Tile(1, 1), which appears in the overlap of two Mystic regions in $C_7(2)$ and $C_6(2)$, are the PO-side. Meanwhile, the other pentagonal patches corresponding to the remaining rhombuses with an acute angle of 30° are the AO-side. In other words, in the second pattern of T_s in the case of $u = 0$, AO-side pentagonal patches can be placed on most rhombuses[9], whereas PO-side pentagonal patches must be placed on some rhombuses with an acute angle of 30°.

In Section 5.4, we explain the reason why Figures 5-5 and 5-6 represent the second pattern, from the same perspective as Figure 4-4 shown for T_h, and discuss the common properties of the second pattern series of T_s in the cases of $u = 0$ and $u \geq 1$.

5.3 Countless patterns of non-periodic tilings that Tile(1, 1) can generate and their conversion

Figure 5-7 shows Type A, Type B, and Type C of $C_7(2)$[10], as explained in Section 4.3 in the previous paper [6]. In [6], we explained that by using these Types, countless patterns (design

[10]Type A in Figure 5-7 corresponds to $C_7(2)$ of T_s in Figure 5-1. Type B and Type C in Figure 5-7 are clusters created by replacing the Mystic regions inside $C_7(2)$ with the Mystic formed by the reflected Tile(1, 1), and their outlines are identical to that of Type A.

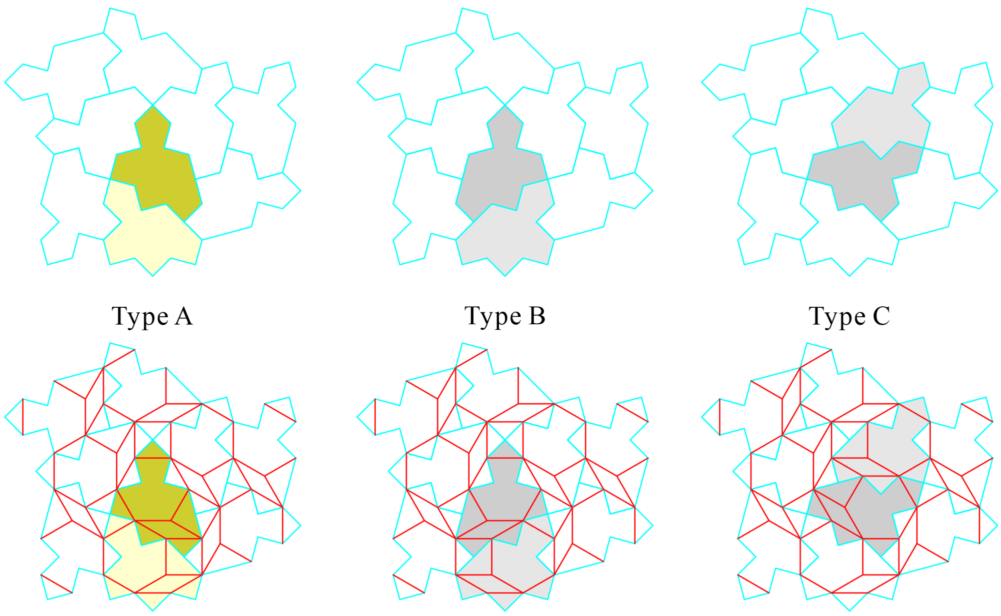

Figure 5-7: $C_7(2)$ and three types of patterns.

patterns created by the arrangement of polygonal tiles) of non-periodic tilings with three types of pentagons based on T_s can be generated, and that the patterns fall into the first and second series. The explanation of the series can be rewritten using the terms "AO-side" and "PO-side," as shown below. In the case of $u = 0$, we assumed that the first pattern series of T_s represents the case in which the pentagonal patch at one of the three locations corresponding to rhombuses with an acute angle of 30°, contained in three Tile$(1,1)$ used in the two Mystic regions in $C_7(2)$ (and $C_6(2)$), is the AO-side, whereas the pentagonal patches at locations corresponding to the other rhombuses with an acute angle of 30° are the PO-side. In the cases of $u = 0$, we assumed that the second pattern series of T_s represents the case in which the pentagonal patch at one of the three locations corresponding to rhombuses with an acute angle of 30° contained in three Tile$(1,1)$ used in the two Mystic regions in $C_7(2)$ (and $C_6(2)$), is the PO-side, whereas the pentagonal patches at locations corresponding to the other rhombuses with an acute angle of 30° are the AO-side.

Even in the case of $u \geq 1$, countless patterns of non-periodic tilings with three types of pentagons based on T_s can be generated by using Type A, Type B, and Type C of $C_7(2)$, and these patterns fall into the first and second series. The clusters for generating them and their properties are shown below by using the case of $u = 1$.

Figure 5-8 presents clusters $FPC_7(2,1)A$, $FPC_7(2,1)B$, and $FPC_7(2,1)C$, which are based on the first pattern corresponding to Types A, B, and C in Figure 5-7. (Note: $FPC_7(2,1)A$ corresponds to $FPC_7(2,1)$ in Figure 5-3. The outlines of $FPC_7(2,1)B$ and $FPC_7(2,1)C$ are identical to that of $FPC_7(2,1)A$). Figure 5-9 presents clusters $SPC_7(2,1)A$, $SPC_7(2,1)B$, and $SPC_7(2,1)C$, which are based on the second pattern corresponding to Types A, B, and C in Figure 5-7. (Note: $SPC_7(2,1)A$ corresponds to $SPC_7(2,1)$ in Figure 5-5. The outlines of $SPC_7(2,1)B$ and $SPC_7(2,1)C$ are identical to that of $SPC_7(2,1)A$).

Based on Figure 5-8, we assume that the first pattern series of T_s in the case of $u \geq 1$ represents the case where PO-side pentagonal patches are placed on the original rhombuses.

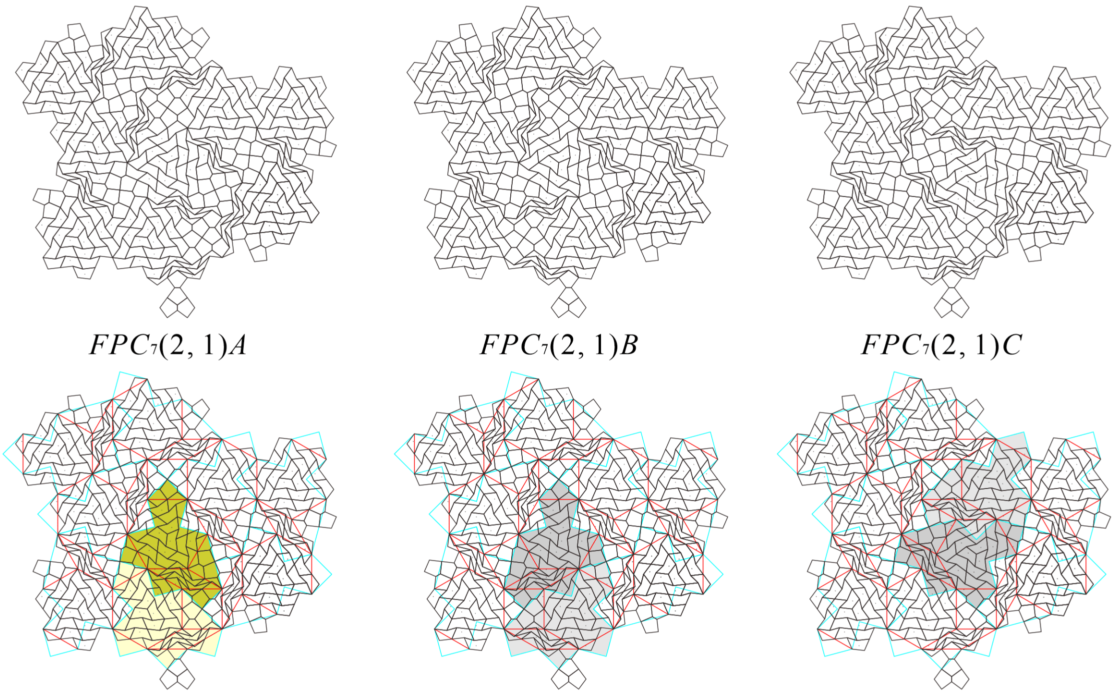

Figure 5-8: $FPC_7(2,1)A$, $FPC_7(2,1)B$, and $FPC_7(2,1)C$.

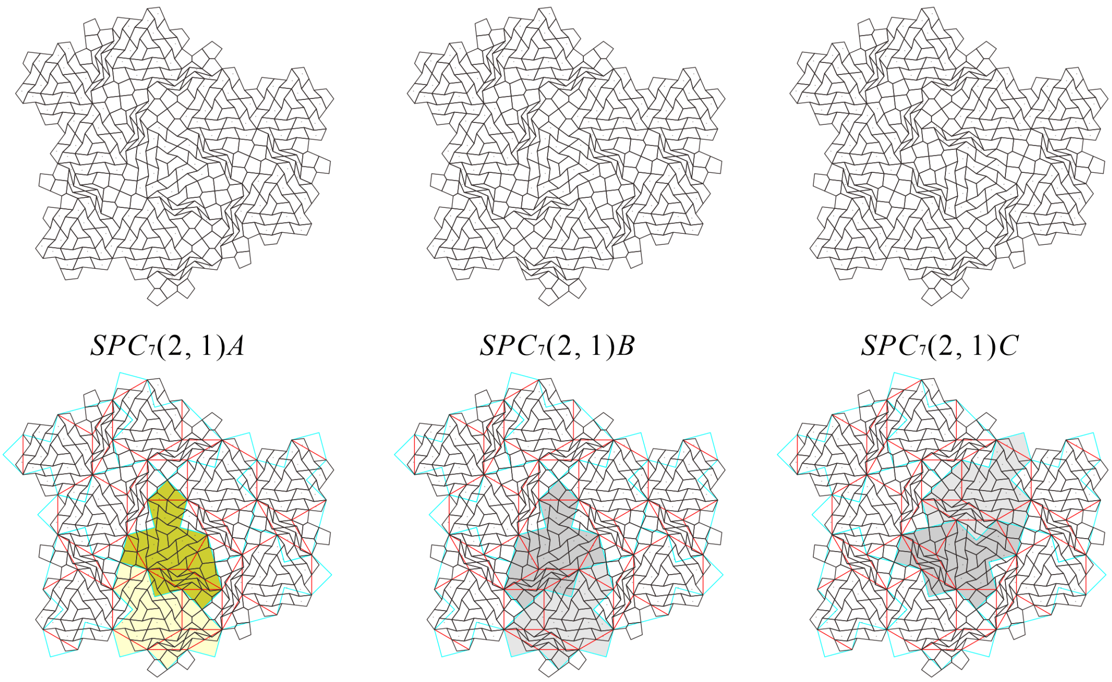

Figure 5-9: $SPC_7(2,1)A$, $SPC_7(2,1)B$, and $SPC_7(2,1)C$

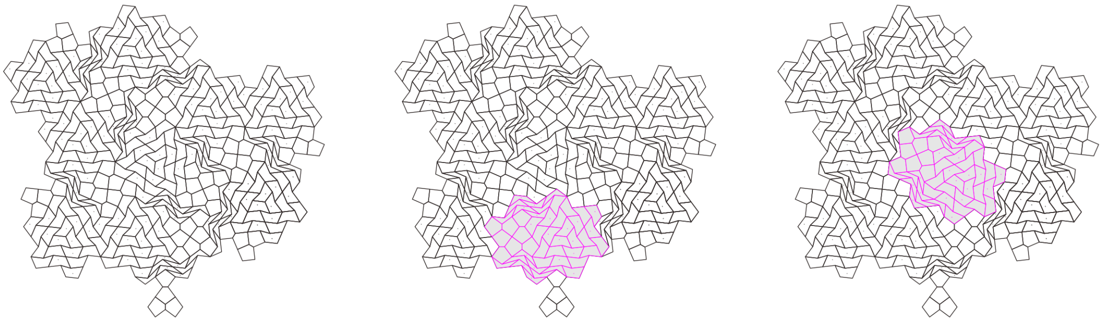

$FPC_7(2,1)A$ $FPC_7(2,1)B$ $FPC_7(2,1)C$

Figure 5-10: Locations where patterns of pentagons changed in $FPC_7(2,1)B$ and $FPC_7(2,1)C$ relative to $FPC_7(2,1)A$.

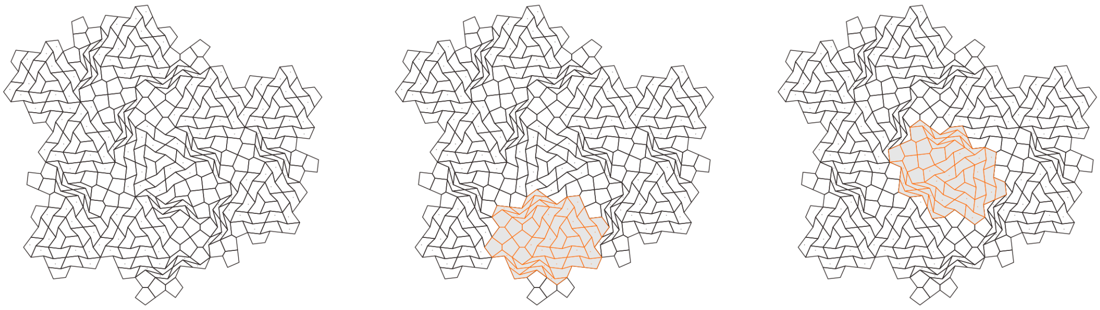

$SPC_7(2,1)A$ $SPC_7(2,1)B$ $SPC_7(2,1)C$

Figure 5-11: Locations where patterns of pentagons changed in $SPC_7(2,1)B$ and $SPC_7(2,1)C$ relative to $SPC_7(2,1)A$.

Based on Figure 5-9, we assume that the second pattern series of T_s in the case of $u \geq 1$ represents the case where AO-side pentagonal patches are placed on the original rhombuses.

Figure 5-10 shows the locations where the pattern of pentagons changed in $FPC_7(2,1)B$ and $FPC_7(2,1)C$ relative to $FPC_7(2,1)A$. The components of these changed locations are identical. Similarly, Figure 5-11 shows the locations where the pattern of pentagons changed in $SPC_7(2,1)B$ and $SPC_7(2,1)C$ relative to $SPC_7(2,1)A$. The components of these changed locations are identical. Note that, as shown in Section 4.3 of [6], in the case of $u = 0$, there were two types of components at the change locations for both the first and second patterns. Figure 5-12 illustrates the components at the change locations for the first and second patterns in the case of $u \geq 1$. The outlines of the components exhibit 180° rotational symmetry and are reflected images of each other. (The locations corresponding to regular hexagons inside them can be replaced. Thus, depending on the pattern of the internal pentagons, the reflected image relationship may not always hold. However, the outlines are always reflected images).

5.4 Classification based on common properties

Figure 5-13 shows the clusters $FPC_7(2)$ (in the case of $u = 0$, see Figure 4-3 in [6]), $FPC_7(2,1)$ (in the case of $u = 1$, see Figure 5-3), and $FPC_7(2,2)$ (in the case of $u = 2$, see Figure 5-4), which are formed by three types of pentagons based on $C_7(2)$. The regions

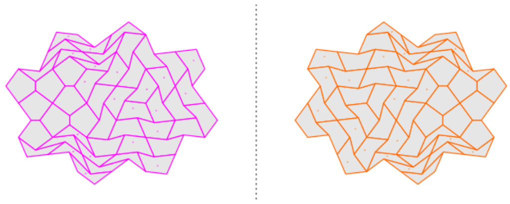

Figure 5-12: Relationship between the components at the change locations in $FPC_7(2,1)B$ and $FPC_7(2,1)C$, and those in $SPC_7(2,1)B$ and $SPC_7(2,1)C$.

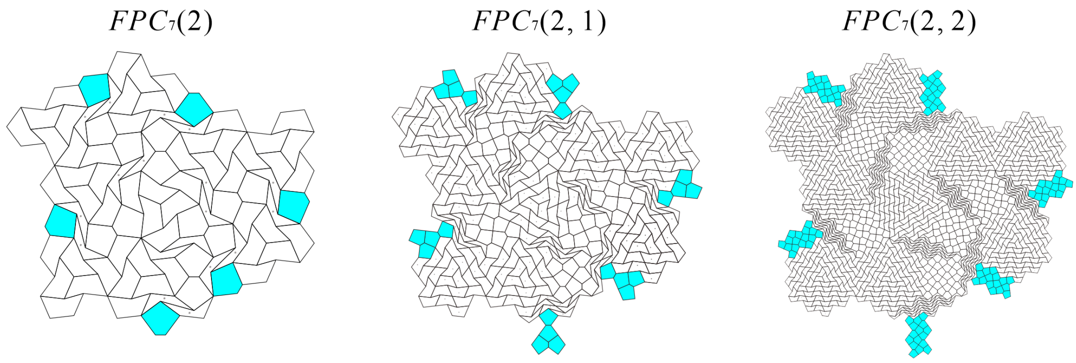

Figure 5-13: Regions on the contours of $FPC_7(2)$, $FPC_7(2,1)$, and $FPC_7(2,2)$ that correspond to the original rhombuses with an acute angle of 90°.

along the contours of these clusters that correspond to the original rhombuses with an acute angle of 90° (which contain only half the number of pentagons) are highlighted in light blue. From Figure 5-13, it is seen that the orientations (contact configurations) of the pentagons in the light blue regions share a common property. Non-periodic tilings generated by clusters exhibiting this common property are classified into the first pattern series of T_s.

Thus, by focusing on the common properties shared between the cases of $u = 0$ and $u \geq 1$, we assume that the first pattern series of T_s represents the case in which the pentagons on the posterior side can be placed at the obtuse angles of most rhombuses (i.e., PO-side pentagonal patches can be placed on most of the original rhombuses)[11].

For the first pattern of T_s with three types of pentagons in the case of $u = 0$, see Figure 4-6 in [6]. Owing to PC specifications and other constraints, it is currently difficult to present figures (equivalent to Figure 4-6 in [6]) depicting the first pattern of T_s with three types of pentagons in the case of $u \geq 1$. Therefore, in Figure A-3 of Appendix A, we provide two types of concave polygons equivalent to the outlines of $FPC_7(2,1)$ and $FPC_6(2,1)$, and present clusters corresponding to $FPC_7(3,1)$ and $FPC_7(4,1)$ (i.e., the next substitution step and its next step clusters) using these polygons.

Figure 5-14 shows the clusters $SPC_7(2)$ (in the case of $u = 0$, see Figure 4-7 in [6]),

[11]We use the phrase "pentagons (patches) can be placed" because we consider the fact that pentagons corresponding to the rhombus with an acute angle of 90° exhibit line symmetry, as well as the fact that the replacement of units formed by three pairs of pentagons on the anterior side and units formed by three pairs of pentagons on the posterior side corresponding to regular hexagons is allowed. We use the phrase "most of" because, in the case of $u = 0$, the pentagonal patch at one of the three locations corresponding to rhombuses with an acute angle of 30°, contained in three Tile(1, 1) used in the two Mystic regions in $C_7(2)$ and $C_6(2)$, must be the AO-side.

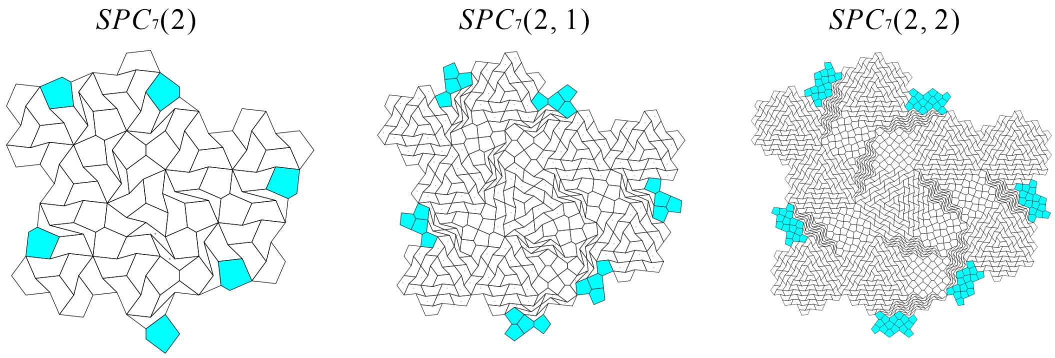

Figure 5-14: Regions on the contours of $SPC_7(2)$, $SPC_7(2,1)$, and $SPC_7(2,2)$ that correspond to the original rhombuses with an acute angle of 90°.

$SPC_7(2,1)$ (in the case of $u = 1$, see Figure 5-5), and $SPC_7(2,2)$ (in the case of $u = 2$, see Figure 5-6), which are formed by three types of pentagons based on $C_7(2)$. The regions along the contours of these clusters that correspond to the original rhombuses with an acute angle of 90° (which contain only half the number of pentagons) are highlighted in light blue. From Figure 5-14, it is seen that the orientations (contact configurations) of the pentagons in the light blue regions share a common property. Non-periodic tilings generated by clusters exhibiting this common property are classified into the second pattern series of T_s.

Thus, by focusing on the common properties shared between the cases of $u = 0$ and $u \geq 1$, we assume that the second pattern series of T_s represents the case in which the pentagons on the anterior side can be placed at the obtuse angles of most rhombuses (i.e., AO-side pentagonal patches can be placed on most of the original rhombuses)[12].

For the second pattern of T_s with three types of pentagons in the case of $u = 0$, see Figure 4-9 in [6]. Owing to PC specifications and other constraints, it is currently difficult to present figures (equivalent to Figure 4-9 in [6]) depicting the second pattern of T_s with three types of pentagons in the case of $u \geq 1$. Therefore, in Figure A-4 of Appendix A, we provide two types of concave polygons equivalent to the outlines of $SPC_7(2,1)$ and $SPC_6(2,1)$, and present clusters corresponding to $SPC_7(3,1)$ and $SPC_7(4,1)$ (i.e., the next substitution step and its next step clusters) using these polygons.

6 Conclusions

Tile(1, 1) can generate countless patterns of tilings if the use of reflected tiles is allowed during the tiling generation process. If Tile(1, 1) is assigned a pattern incorporating decomposition lines, as shown in Figure 1-1, then the tilings with Tile(1, 1) can also be converted into edge-to-edge tilings consisting of squares, regular hexagons, and rhombuses with an acute angle of 30°. Consequently, because a regular hexagon can be divided into three rhombuses with an acute angle of 60°, the tilings with Tile(1, 1) can be converted into edge-to-edge tilings consisting of rhombuses with acute angles of 90°, 60°, and 30°. Therefore, they can also be converted into tilings with three types of pentagons. Additionally, because a rhombus can be

[12]The reasons why for using the phrase "pentagons (patches) can be placed" is the same as that stated in footnote 11. We use the phrase "most of" because, in the case of $u = 0$, the pentagonal patch at one of the three locations corresponding to rhombuses with an acute angle of 30°, contained in three Tile(1, 1) used in the two Mystic regions in $C_7(2)$ and $C_6(2)$, must be the PO-side.

divided into its own similar figures, they can also be converted into tilings with three types of pentagons after subdividing the original rhombus into smaller similar rhombuses[13].

For the non-periodic tilings T_h and T_s with Tile$(1,1)$, the common properties of the conversion results into tilings with three types of pentagons, both with and without subdivision of the original rhombus into smaller similar rhombuses, are shown below. When arbitrary replacements—namely, the arbitrary replacements of locations corresponding to regular hexagons and to the structure of Mystic in T_s—are excluded, the non-periodic tilings with three types of pentagons corresponding to T_h and T_s with Tile$(1,1)$ exhibit two distinct patterns each. Furthermore, when the arbitrary replacement of locations corresponding to the structure of Mystic in T_s is allowed, countless patterns of non-periodic tilings with three types of pentagons corresponding to T_s fall into two distinct series.

Note that when the non-periodic tiling T_s with Tile$(1,1)$ is converted into non-periodic tilings with three types of pentagons, clearly different properties in the orientation of the pentagons are observed between the resulting pentagonal tilings obtained with and without subdivision of the original rhombus into smaller similar rhombuses (see Section 5).

References

[1] Grünbaum, B. and Shephard, G. C. (1987). *Tilings and Patterns*. W. H. Freeman and Company, New York, pp.15–56 (Chapter 1), pp.471–518 (Chapter 9), pp.520–582 (Chapter 10).

[2] Smith, D., Myers, J. S., Kaplan, C. S., and Goodman-Strauss, C. (2024). An aperiodic monotile. *Combinatorial Theory*, **4**(1), 1–91. doi:10.5070/C64163843

[3] Smith, D., Myers, J. S., Kaplan, C. S., and Goodman-Strauss, C. (2024). A chiral aperiodic monotile. *Combinatorial Theory*, **4**(2), 1–25. doi:10.5070/C64264241

[4] Sugimoto, T. (2020). Pentagons and rhombuses that can form rotationally symmetric tilings. arXiv:2005.12709 (accessed on 16 May 2025).

[5] Sugimoto, T. (2022). Converting tilings with multiple types of rhombuses to pentagonal tilings. arXiv:2203.04457 (accessed on 16 May 2025).

[6] Sugimoto, T. (2023). Converting non-periodic tiling with Tile$(1,1)$ into tilings with three types of pentagons, I, arXiv:2307.08184 (accessed on 16 May 2025).

[7] Sugimoto, T., Supplement of the paper "Converting non-periodic tiling T_s with Tile$(1,1)$ into tilings with three types of pentagons," `https://tilingpackingcovering.web.fc2.com/Ts_with_3-types_pentagons-e.html` (accessed on 16 May 2025).

[8] Sugimoto, T., Supplement of the paper "Converting non-periodic tiling T_h with Tile$(1,1)$ into tilings with three types of pentagons," `https://tilingpackingcovering.web.fc2.com/Th_with_3-types_pentagons-e.html` (accessed on 16 May 2025).

Appendix A

For the case of $u = 1$, we provide supplementary figures that illustrate the conversion of the non-periodic tilings T_h and T_s with Tile$(1,1)$ into tilings with three types of pentagons.

[13] Tile$(1,1)$ can generate a variety of patterns of periodic tilings. These periodic tilings with Tile$(1,1)$ can be converted in a similar manner for the case of non-periodic tilings T_h and T_s (see Appendix B) [6].

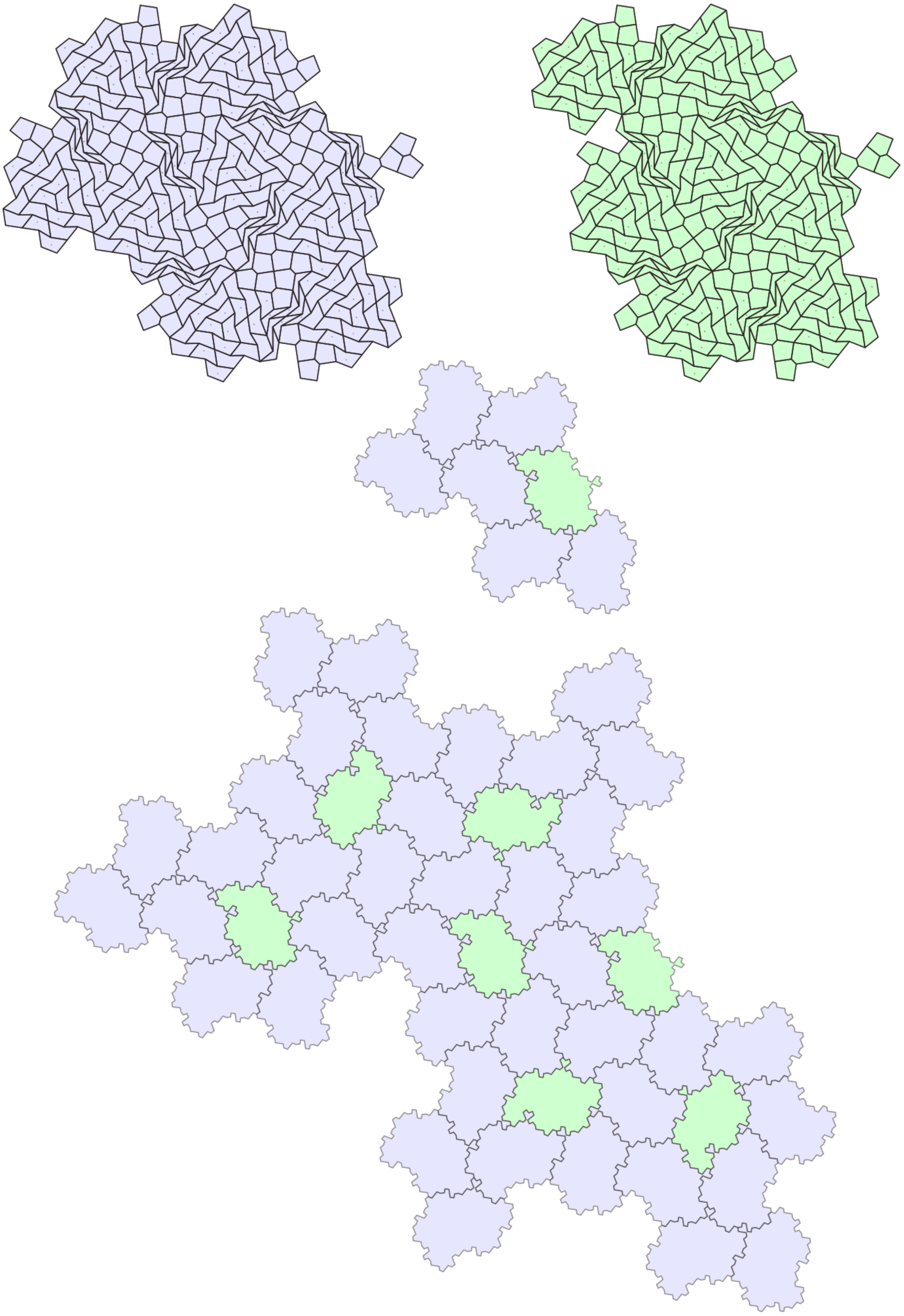

Figure A-1: Clusters $FPH_8(2,1)$ and $FPH_7(2,1)$, along with clusters corresponding to $FPH_8(3,1)$ and $FPH_8(4,1)$, represented using two types of concave polygons that are equivalent to the outlines of $FPH_8(2,1)$ and $FPH_7(2,1)$.

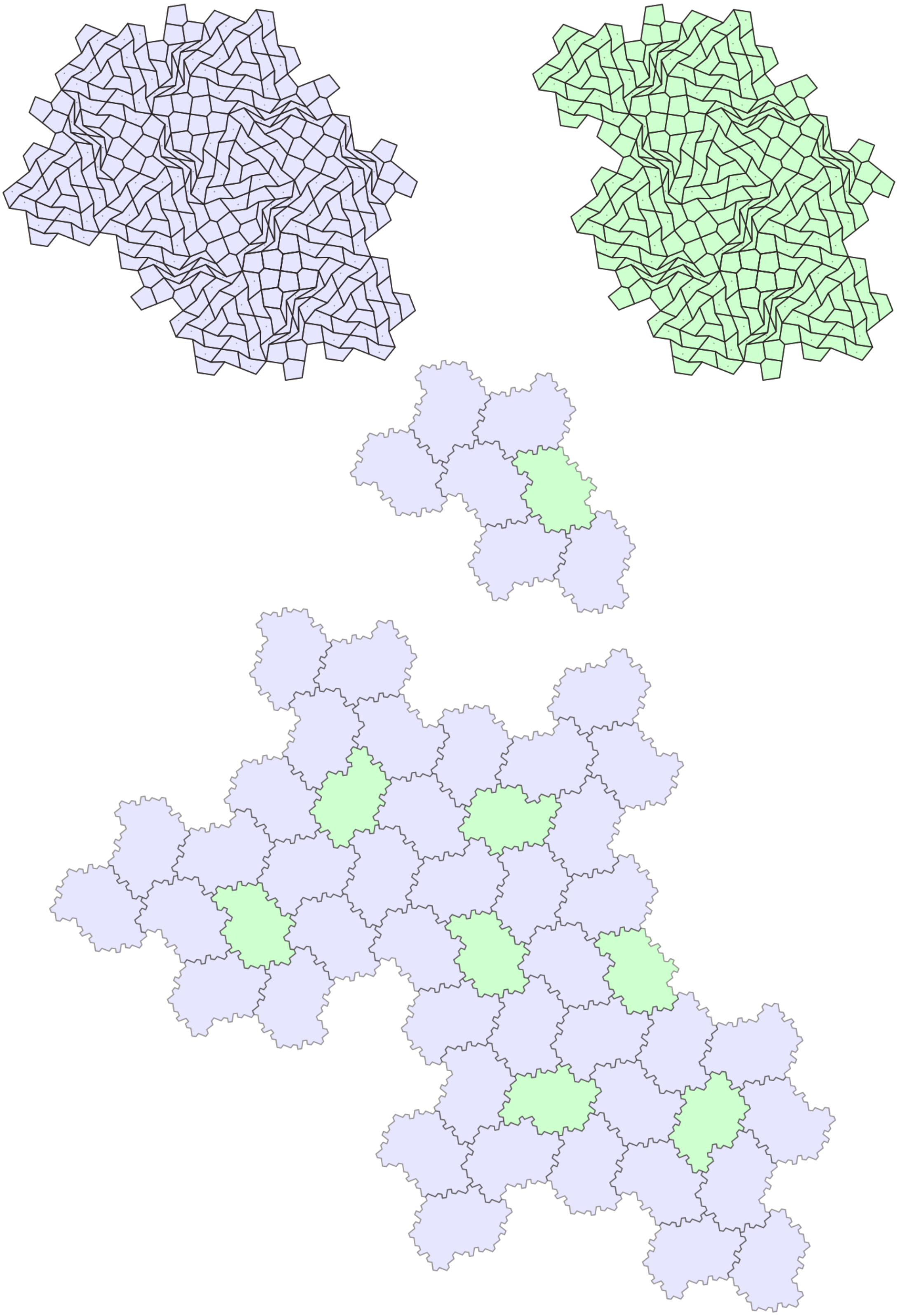

Figure A-2: Clusters $SPH_8(2,1)$ and $SPH_7(2,1)$, along with clusters corresponding to $SPH_8(3,1)$ and $SPH_8(4,1)$, represented using two types of concave polygons that are equivalent to the outlines of $SPH_8(2,1)$ and $SPH_7(2,1)$.

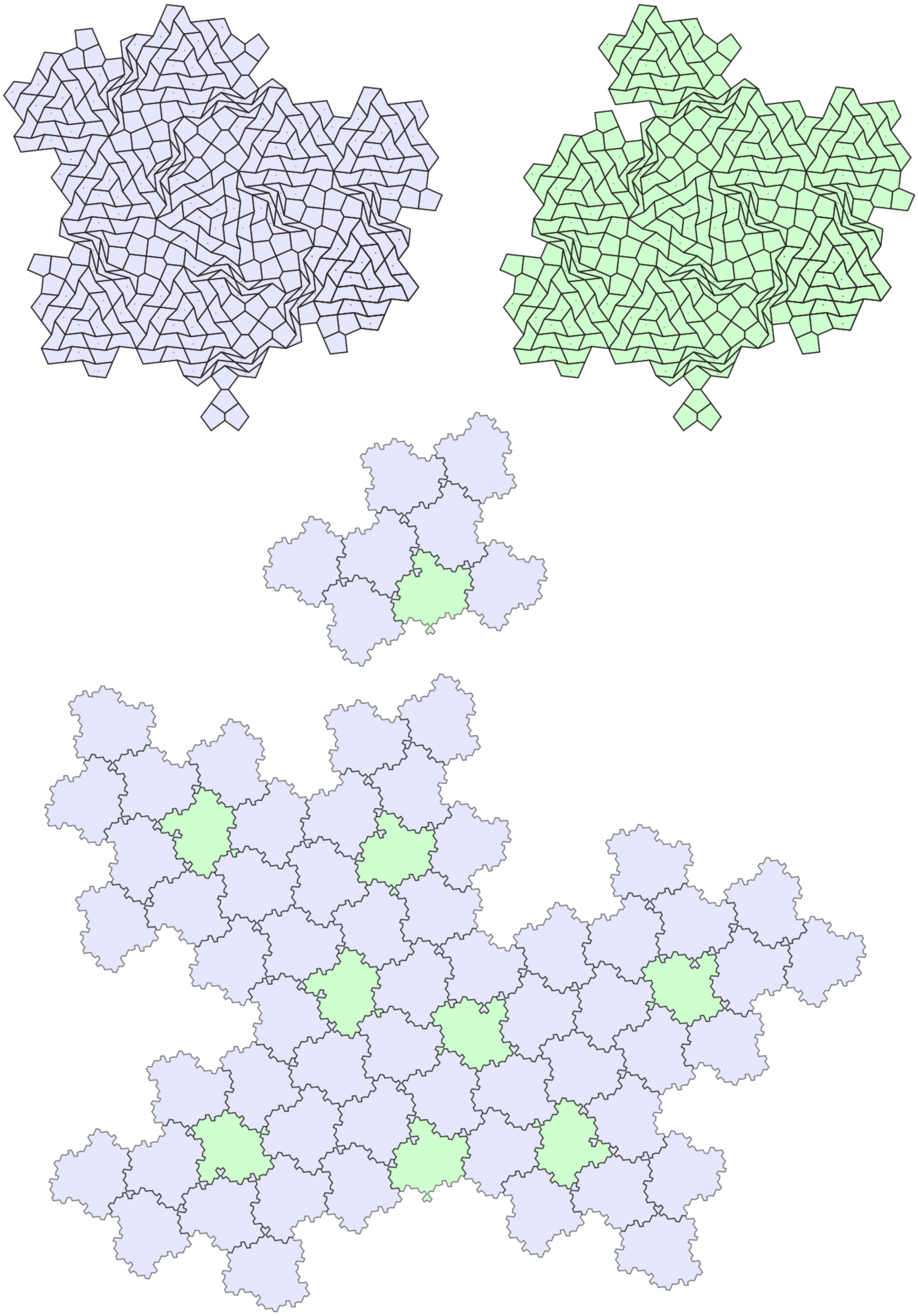

Figure A-3: Clusters $FPC_7(2,1)$ and $FPC_6(2,1)$, along with clusters corresponding to $FPC_7(3,1)$ and $FPC_7(4,1)$, represented using two types of concave polygons that are equivalent to the outlines of $FPC_7(2,1)$ and $FPC_6(2,1)$.

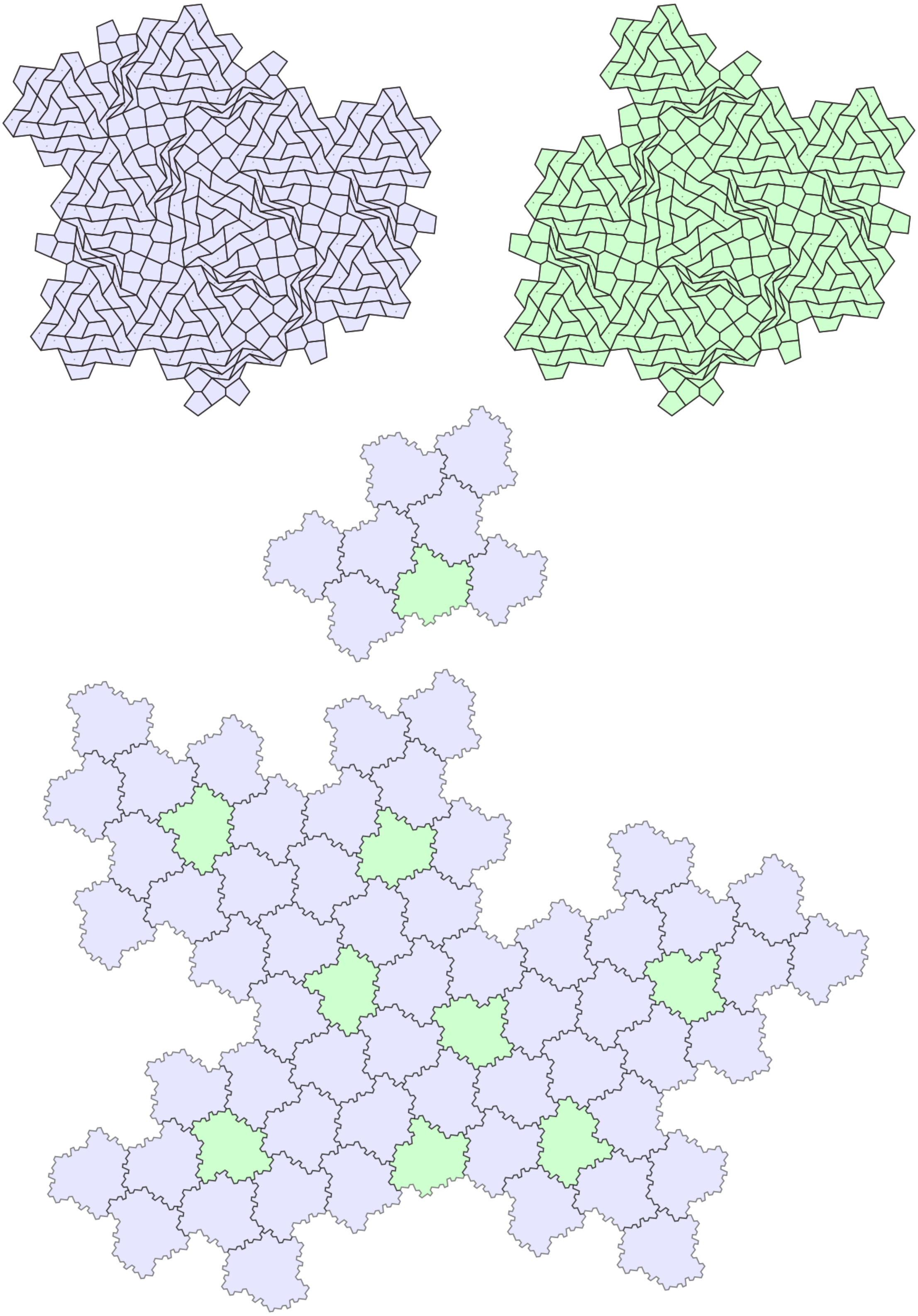

Figure A-4: Clusters $SPC_7(2,1)$ and $SPC_6(2,1)$, along with clusters corresponding to $SPC_7(3,1)$ and $SPC_7(4,1)$, represented using two types of concave polygons that are equivalent to the outlines of $SPC_7(2,1)$ and $SPC_6(2,1)$.

Appendix B

As mentioned in Appendix B of the previous paper [6], Tile(1, 1) can generate a variety of patterns of tilings by combining bands of two types of translation units (units that can generate periodic tilings through translation alone). However, if the decomposition line pattern shown in Figure 1-1 is applied to Tile(1, 1) forming tilings of those patterns, it can be converted into a periodic tiling consisting of squares, regular hexagons, and rhombuses with an acute angle of 30° shown in Figure B-1. In [6], the tiling that represents the structural pattern in Figure B-1 was defined as T_p. Thus, T_p with Tile(1, 1) can be converted into an edge-to-edge tiling consisting of rhombuses with acute angles of 90°, 60°, and 30°. It can also be converted into tilings with three types of pentagons.

Figures B-2 and B-3 show periodic tilings with three types of pentagons corresponding to T_p, formed by PO-side pentagonal patches in the cases of $u = 1$ and $u = 2$, respectively. Figures B-4 and B-5 show periodic tilings with three types of pentagons corresponding to T_p, formed by AO-side pentagonal patches in the cases of $u = 1$ and $u = 2$, respectively.

By comparing the tilings in Figures B-2 and B-4, we observe the reflected counterpart of the translation unit formed by the pentagonal patches on the AO-side in the tiling formed by the pentagonal patches on the PO-side, as shown in Figure B-6. Similarly, by comparing the tilings in Figures B-3 and B-5, we observe the reflected counterpart of the translation unit formed by the pentagonal patches on the AO-side in the tiling formed by the pentagonal patches on the PO-side, as shown in Figure B-7. Note that, because the pentagonal patches corresponding to regular hexagons can be arbitrarily replaced, the reflected counterpart of the translation unit may not always be directly superimposable, depending on the patterns within the pentagonal patches. However, by adjusting the patterns within the pentagonal patches, it is possible to find a location within the tiling where the reflected counterpart of the translation unit can be perfectly superimposed.

As shown in the previous paper [6], when the arbitrary replacements of locations corresponding to regular hexagons are excluded, the tilings with three types of pentagons corresponding to T_p in the case of $u = 0$ exhibit two patterns. Conversely, when the arbitrary replacements of locations corresponding to regular hexagons are excluded, the tilings with three types of pentagons corresponding to T_p in the case of $u \geq 1$ exhibit a single pattern.

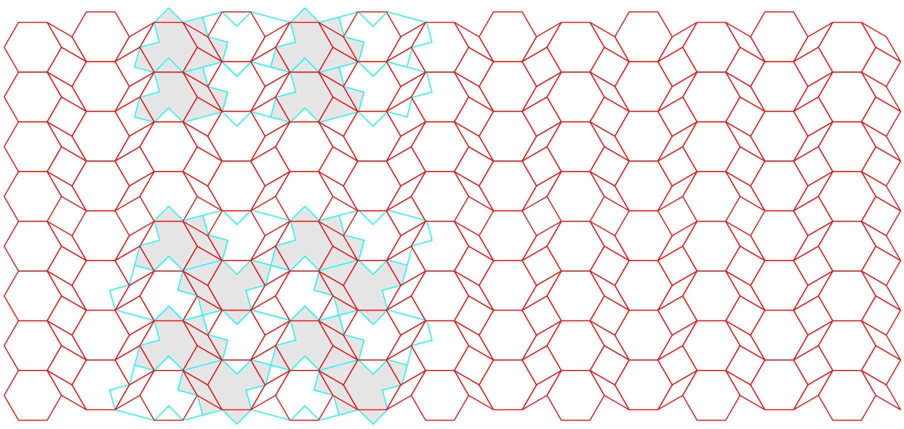

Figure B-1: Periodic tiling T_p formed by squares, regular hexagons, and rhombuses with an acute angle of 30°.

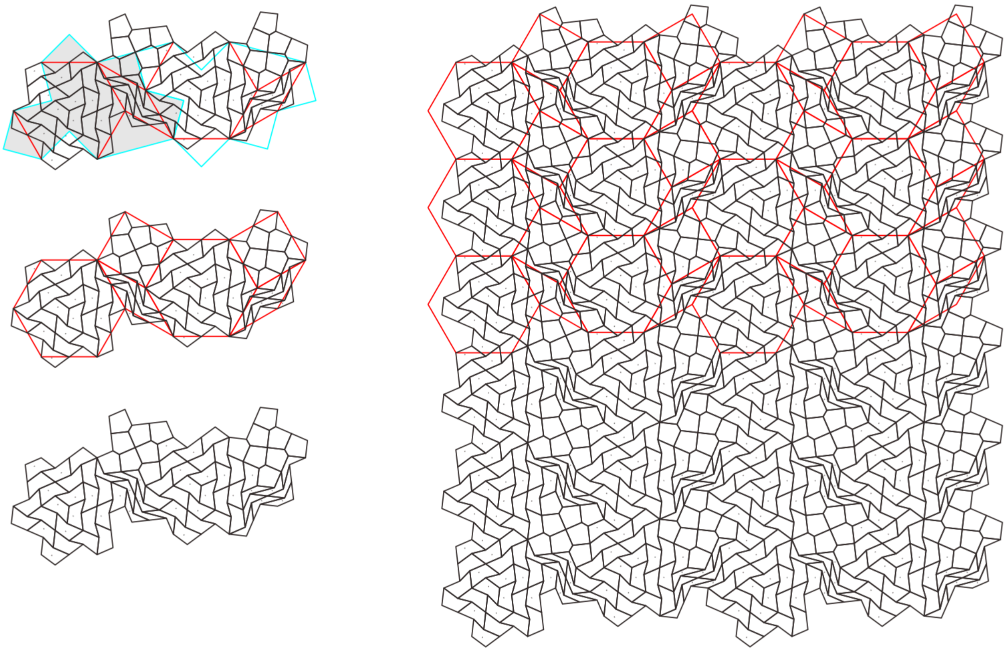

Figure B-2: T_p formed by PO-side pentagonal patches in the case of $u = 1$.

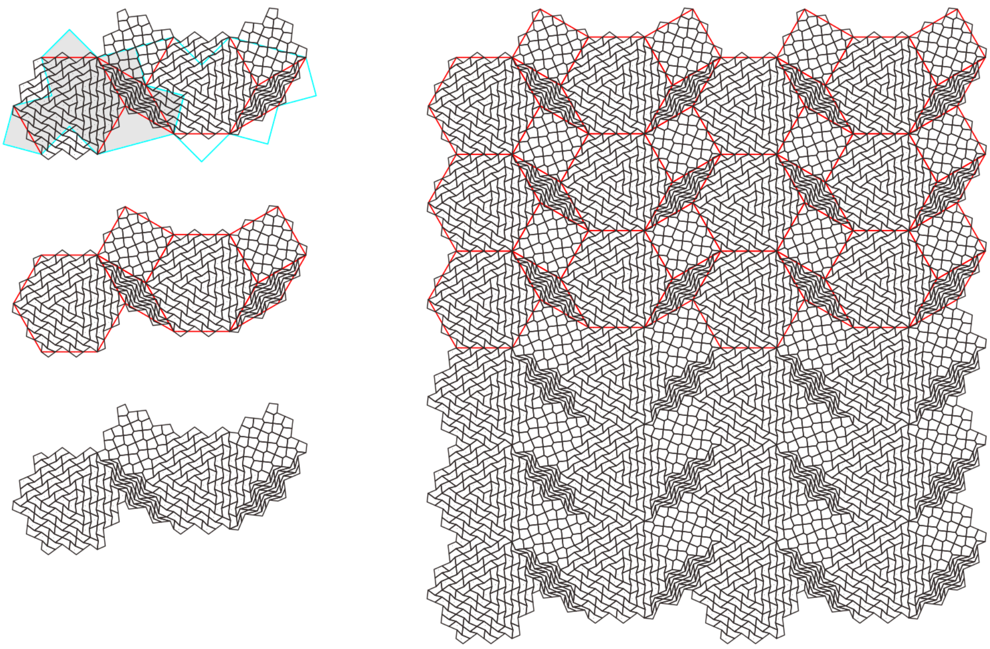

Figure B-3: T_p formed by PO-side pentagonal patches in the case of $u = 2$.

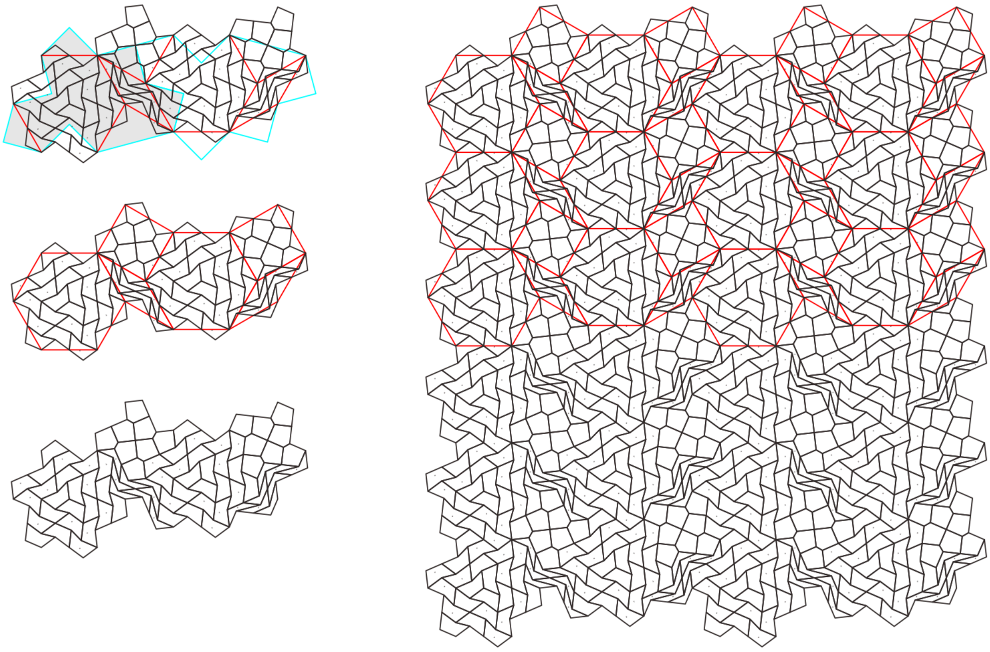

Figure B-4: T_p formed by AO-side pentagonal patches in the case of $u = 1$.

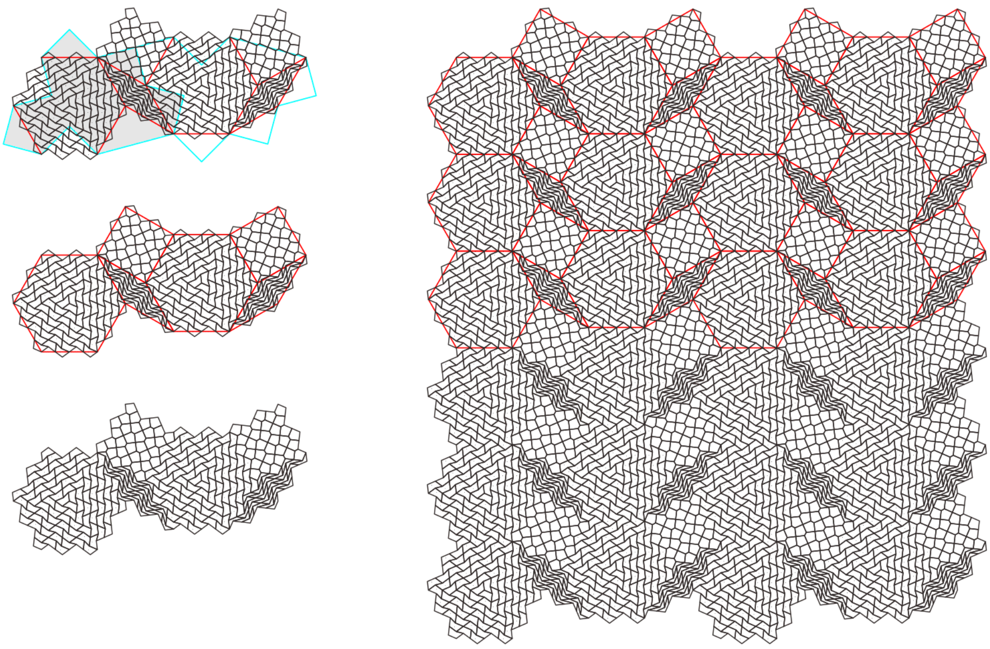

Figure B-5: T_p formed by AO-side pentagonal patches in the case of $u = 2$.

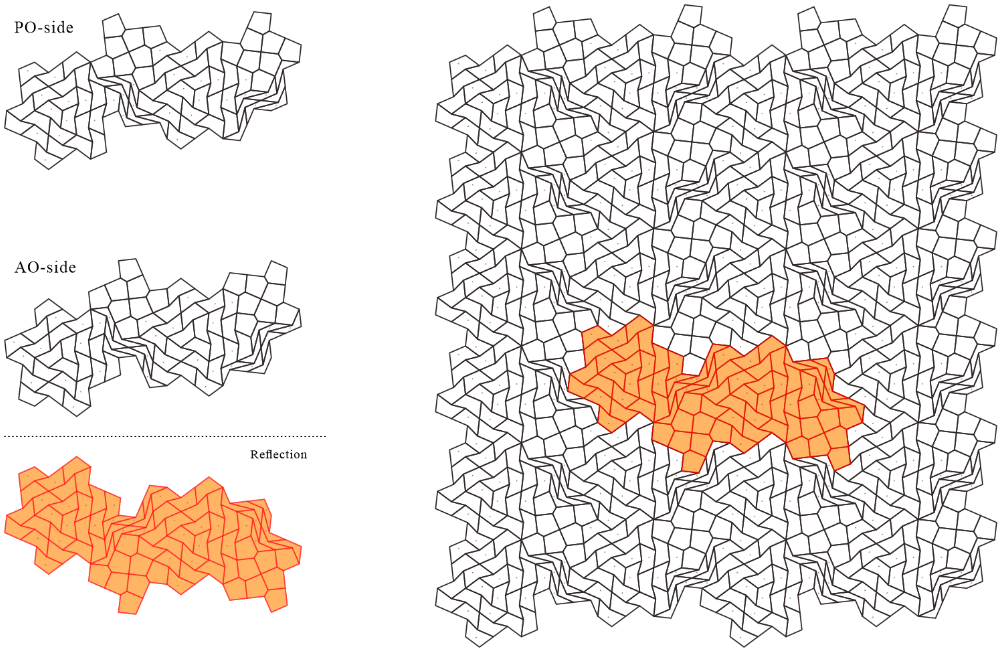

Figure B-6: Confirmation that T_p formed by pentagonal patches on the PO-side and AO-side in the case of $u = 1$ has the same pattern.

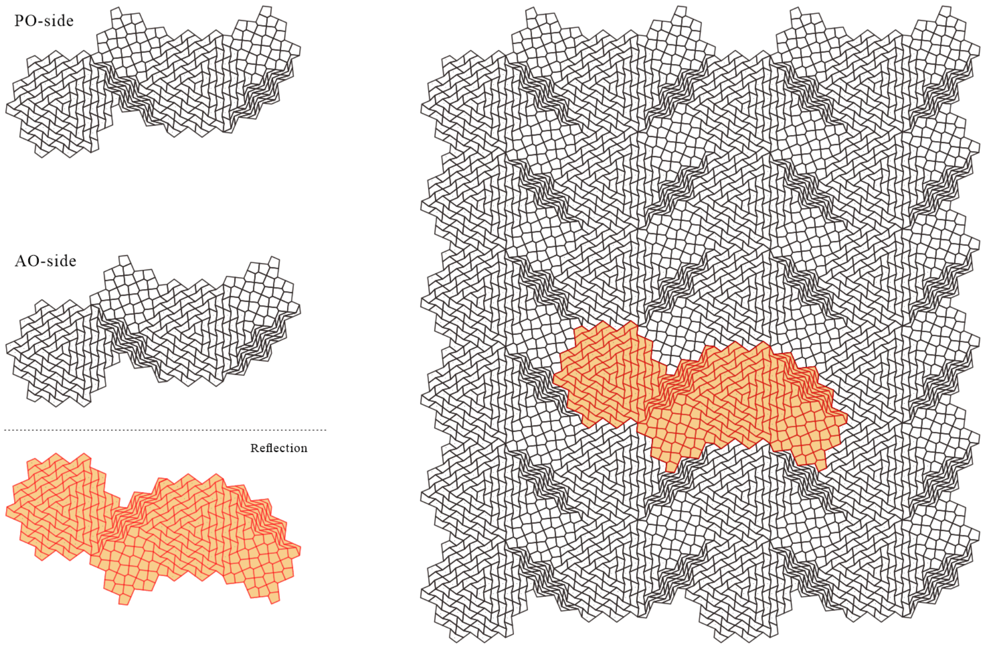

Figure B-7: Confirmation that T_p formed by pentagonal patches on the PO-side and AO-side in the case of $u = 2$ has the same pattern.

Appendix C

Errata: There is an error in the manuscript v3 of [6].

P.25, lines 2–4 below Figure B-4:

T_p with Tile$(1, 1)$ can be converted into non-periodic tilings consisting of rhombuses with acute angles of 90°, 60°, and 30°.

should be changed to

T_p with Tile$(1, 1)$ can be converted into an edge-to-edge tiling consisting of rhombuses with acute angles of 90°, 60°, and 30°.